SIAM J. Applied Dynamical Systems
Vol. 21, No. 1, pp. 470–499

Bifurcation Sequences in a Discontinuous Piecewise-Smooth Map Combining Constant-Catch and Threshold-Based Harvesting Strategies*

Cristina Lois-Prados† and Frank M. Hilker‡

Abstract. We consider a harvesting strategy that allows constant catches if the population size is above a certain threshold value (to obtain predictable yield) and no catches if the population size is below the threshold (to protect the population). We refer to this strategy as threshold constant-catch (TCC) harvesting. We provide analytical and numerical results when applying TCC to monotone population growth models. TCC remedies the tendency to fishery collapse of pure constant-catch harvesting and provides a buffer for quotas larger than the maximum sustainable yield. From a dynamical systems point of view, TCC gives rise to a piecewise-smooth map with a discontinuity at the threshold population size. The dynamical behavior includes border-collision bifurcations, basin boundary metamorphoses, and boundary-collision bifurcation. We further find Farey trees, a slightly modified truncated skew tent map scenario, and the bandcount incrementing scenario. Our results underline, on the one hand, the protective function of thresholds in harvest control rules. On the other hand, they highlight the dynamical complexities due to discontinuities that can arise naturally in threshold-based harvesting strategies.

Key words. nonsmooth discrete one-dimensional dynamical system, discontinuous difference equation, border-collision bifurcation, fishery model, population harvesting, harvest control rule

AMS subject classifications. 92D25, 37E05, 39A28, 39A60

DOI. 10.1137/21M1416515

1. Introduction.

Overexploitation of natural populations remains a major problem worldwide. 72% of the more than 8,000 species on the IUCN Red List are overexploited, for example through hunting, fishing, logging, or collecting species from the wild [43]. Industrial fishing occurs in more than half of the world's ocean area, which amounts to an area more than four times that of terrestrial agriculture [37]. In order to prevent overexploitation, many fisheries are managed on the basis of thresholds [25, 47, 33]. These are population sizes, or spawning stock biomasses, below which harvesting is curtailed or suspended so that the population can gradually recover. They are also called biological reference points [42, 12].

The dynamics of single-species fisheries may be described mathematically by one-dimensional discrete-time maps. If the harvesting is based on threshold population sizes, the map

*Received by the editors April 30, 2021; accepted for publication (in revised form) by M. Chaves December 1, 2021; published electronically February 10, 2022.
https://doi.org/10.1137/21M1416515
Funding: The first author's work was partially supported by PhD scholarship FPU18/00719 (Ministerio de Ciencia, Innovación y Universidades, Spain) and research grants MTM2016-75140-P (AEI/FEDER, UE), ED431C 2019/02 (Xunta de Galicia). Osnabrück University provided funding to the first author to visit the Institute of Environmental Systems Research for a period of six weeks, during which parts of this work were completed.
†Instituto de Matemáticas, Universidade de Santiago de Compostela, Campus Vida, 15782 Santiago de Compostela, Spain (cristina.lois.prados@usc.es).
‡Institute of Environmental Systems Research and Institute of Mathematics, School of Mathematics/Computer Science, Osnabrück University, D–49076 Osnabrück, Germany (frank.hilker@uni-osnabrueck.de).

will be composed of different branches (corresponding to high or low/no harvesting) defined on intervals which are separated at the threshold points (also called break points in the dynamical systems literature). As the map is not differentiable at the threshold points, this gives rise to piecewise-smooth dynamical systems (see, e.g., [13, 3]). They can exhibit so-called nonsmooth bifurcations that differ substantially from those that occur in smooth dynamical systems [14, 4], e.g., border-collision bifurcations [46]. Nonsmooth bifurcations are related to invariant sets colliding with a break point, which is given by the harvesting threshold. In recent years, a lot of progress has been made in understanding the dynamics of piecewise-smooth maps (see, e.g., [4, 21, 57, 48]). However, even though they emerge quite naturally in the context of threshold-based harvesting, their mathematical analysis in the context of fishery models is just at the beginning [5, 16, 17, 28, 29, 40, 52, 53].

Here, we study a harvest control rule that induces a discontinuity at the threshold point. Our results will show that this gives rise to highly complex dynamics, including multiple attractors, different periodic cycles, homoclinic orbits, and even chaotic oscillations. The bifurcations in which these dynamical patterns emerge and disappear involve border- and boundary-collision bifurcations as well as basin boundary metamorphoses. Hence, the discontinuity in the harvest control rule produces rich dynamics that, to our knowledge, have not been observed in continuous harvesting maps. This is particularly true for population maps that are monotone in the absence of harvesting.

The harvesting strategy we consider takes constant catches above the threshold population size and no harvest below the threshold. We shall refer to this policy as *threshold constant-catch (TCC)*. Pure constant-catch (CC) removes a constant amount of yield from the population per unit time. According to Fryxell, Sinclair, and Caughley, CC strategies used to be the norm "in the not-so-distant past" (see [19, p. 330]). As they lack a feedback mechanism to respond to changes in population size, they are considered to increase the risk of stock depletion and crashes, especially in variable environments [9, 26, 41, 20]. On the other hand, one of their main advantages are quotas that remain unchanged or vary very little. Managers frequently propose yield-stabilizing measures so as to achieve more predictable conditions for industry and to reduce capital costs to change production capacity; see [44] and section 3.5.17 of [31]. The economic advantage in stabilizing yield variations may even outweigh greater yields obtained from alternative control rules [11, 45]. Moreover, constant catches have also been argued for in data-poor situations or as part of indicator-based management [32, 36, 55]. Hence, CC policies may be attractive from an economic, transparency, and implementation point of view. Yet, it has been argued that they "should include some mechanisms to reduce removals if there are signals of stock depletion" (see [55, p. 701]).

The rationale for the TCC strategy is to augment the catch-stabilizing CC strategy with a threshold point to protect the stock if it is below the threshold. Threshold-based strategies are considered more protective and precautionary. In general, above the threshold several harvesting strategies are possible, e.g., harvesting the entire excess (fixed escapement; see [8, 38, 29]), a proportion of the excess (proportional threshold harvesting; see [15, 35, 28]), or a proportion of the population (threshold policy; see [51, 5]).

CC strategies above the threshold are referred to as *conditional constant-catch* strategies in

[12].[1] Mathematical and simulation models of such strategies are relatively rare and scattered in the literature [7, 30, 10, 2, 56, 49, 40]. To our knowledge, the TCC strategy has been considered so far only in a slightly different form in [2] and as a special case in [30]; see subsection 2.3 for more details. A related strategy, called precautionary threshold constant-catch (PTCC) harvesting [40], removes the discontinuity at the threshold point by gradually increasing the allowed harvest until the CC level is reached. The PTCC strategy will serve as a baseline, against which we can compare the effects induced by the discontinuity. Figure 1 shows an illustration of CC harvesting, PTCC, and TCC.

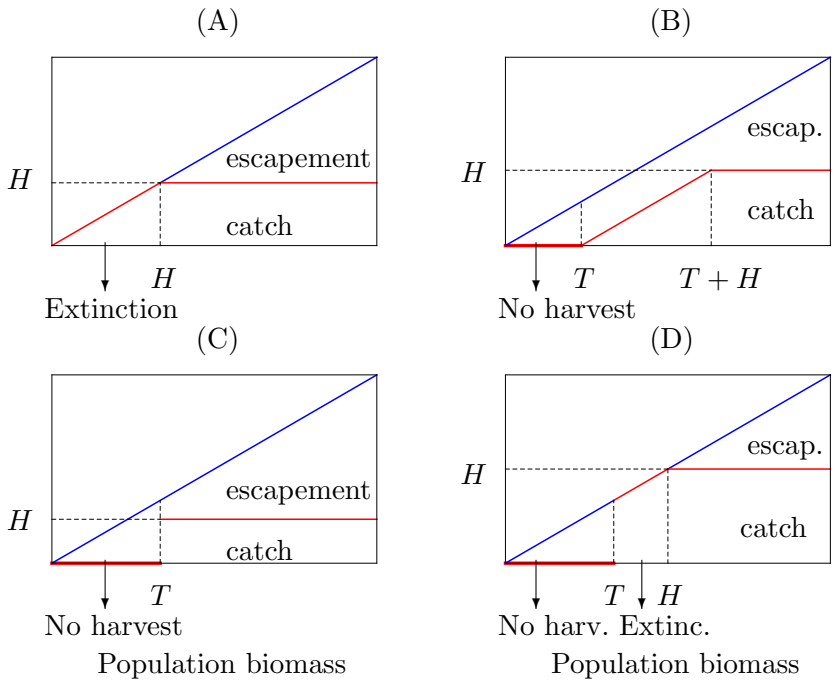

Figure 1. *Different harvesting strategies which make use of constant catches. We represent the catch (red solid line) as a function of the population biomass. The blue line represents the identity map, T is the threshold, and H is the maximum allowed quota.* (A) *CC harvesting;* (B) *PTCC harvesting. The bottom panels show TCC harvesting with* (C) $H < T$ *and* (D) $H > T$.

In this paper, we use single-species difference equations with monotone stock-recruitment relationships as generic undercompensatory population models. We study the influence of the harvest control parameters on population dynamics, average yield, and harvest frequency. The paper is organized as follows. Section 2 introduces the model and its underlying assumptions. It also compares TCC with similar control rules. Section 3 briefly recaps definitions of stability and bifurcations, with special attention to those related with piecewise-smooth maps. In section 4, we provide analytical results on the stability of fixed points and the existence of intervals which do not contain any equilibrium and attract long-term dynamics. In section 5, we combine the rigorous results provided in the previous section with simulations from

[1] But it should be noted that this term was used in [10] for a specific harvest strategy for Pacific halibut with CC harvesting above the threshold and proportional harvesting below the threshold.

numerical one-parameter bifurcation diagrams to describe the different types of bifurcations, most of them due to the discontinuity character of TCC. In sections 6 and 7, we vary the harvest control parameters to obtain one-parameter and two-parameter bifurcation diagrams. Finally, in section 8 we discuss the results in the context of population dynamics and harvesting management, paying special attention to those features induced by the discontinuity points.

2. Model description.

In this section, we first state some basic assumptions underlying our mathematical model, and we provide the mathematical expression for the TCC control rule. In subsection 2.2, we consider the CC harvesting rule as a particular case. In subsection 2.3, we compare the TCC rule with three similar strategies.

2.1. Threshold constant-catch harvesting strategy.

We consider a single-species population and assume that its growth in the absence of harvesting is governed by the following one-dimensional difference equation:

$$x_{n+1} = f(x_n), \tag{2.1}$$

where x_n denotes the population size (or biomass) at the nth generation, $n = 0, 1, 2, \ldots$, starting at an initial value $x_0 > 0$. The map f is the production or stock-recruitment curve, for which we assume the following conditions typical of monotone population models:

(A) $f : [0, \infty) \longrightarrow [0, \infty)$ is a $\mathcal{C}^2$ map and has a unique positive fixed point $K > 0$, $f(x) > x$ for all $x \in (0, K)$, and $f(x) < x$ for all $x > K$. Moreover, $f(0) = 0$, there exists $\lim_{x\to\infty} f(x) < \infty$, and $f'(x) > 0$, $f''(x) < 0$ for all $x \in [0, \infty)$.

It is widely known that a population governed by a map f under condition **(A)** satisfies that the positive fixed point K is globally asymptotically stable. Condition **(A)** excludes overcompensation and Allee effects. A prominent example of monotone population maps is the Beverton–Holt model

$$z_{n+1} = \frac{rz_n}{1 + az_n},$$

where $r, a \in (0, \infty)$ and z_n denotes the population size at time step n, $n = 0, 1, 2, \ldots$. Applying the change of variables $x_n = az_n$, we obtain the difference equation:

$$x_{n+1} = \frac{rx_n}{1 + x_n}. \tag{2.2}$$

The Beverton–Holt map defined by $f(x) = rx/(1 + x)$ fulfils condition **(A)** for $r > 1$, with $K = r - 1$ and $\lim_{x\to\infty} f(x) = r$. We will use it for the numerical simulations in this paper, but remark that many of our analytical results hold for more general maps satisfying condition **(A)**.

When harvesting a population that is growing according to (2.1) with the TCC rule, we obtain

$$x_{n+1} = F(x_n) := \begin{cases} f(x_n), & f(x_n) < T, \\ \max\{0, f(x_n) - H\}, & f(x_n) \geq T. \end{cases} \tag{2.3}$$

Note that we assume that population size is measured after harvesting in time step t and before reproduction in time step $t+1$. The TCC rule in (2.3) means that there is no harvesting if the

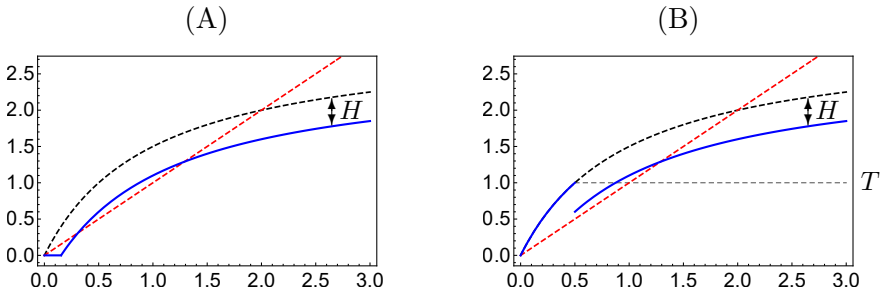

Figure 2. *Illustration of the graph of the map F (blue solid line). The black dashed curve is the Beverton–Holt map with $r = 3$, and the red dashed line is $y = x$.* (A) *CC harvesting, where F is piecewise-smooth continuous with $T = 0, H = 0.4$.* (B) *TCC harvesting, where F is piecewise-smooth discontinuous with $T = 1, H = 0.4$.*

population size (after reproduction) is below a threshold level $T \geq 0$. Above the threshold, the population is harvested with a CC strategy, where $H \geq 0$ is the maximum allowed harvesting quota. Equation (2.3) is a piecewise-smooth map with a discontinuity at the threshold. We will see that the discontinuity drives complex dynamics and that the threshold corresponds to a break point in terms of bifurcation theory (see section 3 for definitions).

Let us consider the map $g(x) = f(x) - H$, $x \in [0, \infty)$; then we can rewrite the map $F : [0, \infty) \longrightarrow [0, \infty)$ in the form

$$F(x) = \begin{cases} f(x), & f(x) < T, \\ 0, & T \leq f(x) < H, \\ g(x), & f(x) \geq \max\{T, H\}. \end{cases} \tag{2.4}$$

The piecewise-smooth map F depends on the two harvesting parameters T and H. The typical shape of F is shown in Figure 2. It is clear that $F \equiv f$ if and only if the harvesting quota vanishes, i.e., $H = 0, T \geq 0$ or the threshold is set too large, i.e., $T > \sup\{f(x),\ x > 0\}, H \geq 0$.

The catch (or yield) obtained in generation n is

$$Y_n = \begin{cases} 0, & f(x_n) < T, \\ \min\{f(x_n), H\}, & f(x_n) \geq T. \end{cases} \tag{2.5}$$

For later reference and convenience of the reader, Table 1 collects the meaning of the main abbreviations and symbols used throughout the paper.

2.2. Constant-catch rule ($T = 0, H > 0$). For later comparison, we state some well-known results for the CC harvesting rule. It is a special case of the TCC strategy (2.3) for $T = 0$ and $H > 0$. The map reads as

$$x_{n+1} = \max\{0, f(x_n) - H\}. \tag{2.6}$$

Its graph is illustrated in Figure 2(A).

The following proposition establishes a critical value H_{20} for the maximum allowed quota. Harvesting above this level ($H > H_{20}$) will drive the population to extinction. Below this level,

Table 1
Main abbreviations and symbols.

Abbreviation/symbol	Meaning
CC	Constant-catch harvesting rule
TCC	Threshold constant-catch harvesting rule
PTCC	Precautionary threshold-constant catch harvesting rule
H	Maximum allowed quota (constant yield)
T	Threshold
f	Population map in the absence of harvesting
g	$g(x) = f(x) - H$: population map with CC harvesting
F	Population map defining TCC
x_n	Population size at generation n
Y_n	Yield at generation n
MSY	Maximum sustainable yield
K	Positive fixed point of f (carrying capacity of the virgin stock)
$\tilde{x}$	Population size sustaining MSY, satisfying $f'(\tilde{x}) = 1$
x^*_-, x^*_+	Positive fixed points of g, i.e., under CC harvesting ($0 < x^*_- \le \tilde{x} \le x^*_+ < K$)
SB	Smooth bifurcation
BCB	Border-collision bifurcation
H_{20}	Fold SB at $H_{20} = f(\tilde{x}) - \tilde{x}$. Corresponds to MSY
H_{10}	Period-adding BCB at $H_{10} = T - \widetilde{x^*_+}$, with $f\left(\widetilde{x^*_+}\right) = T$
H_{12}	Existence BCB at $H_{12} = T - \widetilde{x^*_-}$, with $f\left(\widetilde{x^*_-}\right) = T$
H_{oscill}	Boundary-collision bifurcation at $H_{\text{oscill}} = f(T) - T$
H^*	Fold SB at H^* for $F^2 = f \circ g$
m	$m = \inf\{x > 0 \,:\, F(x) = 0\}$ ($T < H$)
M	$M = \sup\{x > 0 \,:\, F(x) = 0\}$ ($T < H$)

the population will survive, provided the initial condition is large enough. The proposition uses that there exists a unique $\tilde{x} > 0$ such that $f'(\tilde{x}) = 1$. This follows from assumption **(A)** and the mean value theorem. Moreover, $\tilde{x} \in (0, K)$. Note that $\tilde{x}$ is the minimum population size, at which the maximum sustainable yield (MSY) can be harvested (see, e.g., [26, 54]). We use the notation H_{20} instead of MSY, because the former indicates a fold bifurcation at which the number of nontrivial fixed points changes from 2 to 0. The value $\tilde{x}$ will play an important role in the study of the dynamics of the harvesting strategies described by (2.3) and (2.6).

Proposition 2.1. *Assume that f satisfies* **(A)** *and that $H > 0$. Then every solution of (2.6) converges to an equilibrium. More specifically, the following hold:*

(a) *If $H < H_{20} := f(\tilde{x}) - \tilde{x}$, then g has two positive equilibria x^*_- and x^*_+ with $0 < x^*_- < \tilde{x} < x^*_+ < K$. While x^*_- is unstable, x^*_+ and 0 are locally asymptotically stable with the basins of attraction (x^*_-, ∞) and $[0, x^*_-)$, respectively.*

(b) *If $H = H_{20}$, then $\tilde{x}$ is the unique positive fixed point of g. The equilibrium $\tilde{x}$ is semi-stable and 0 locally asymptotically stable with the basins of attraction $[\tilde{x}, \infty)$ and $[0, \tilde{x})$, respectively.*

(c) *If $H > H_{20}$, then g has no positive fixed points and 0 is GAS.*

The results stated in Proposition 2.1 are well known, and their proof follows from elementary arguments, such as the mean value theorem and results for bounded increasing/decreasing sequences.

2.3. Related harvesting strategies. First, we point out that [2] proposed a harvesting strategy very similar to TCC. It reads as

$$x_{n+1} = \begin{cases} f(x_n), & x_n < x_{\text{th}}, \\ f(x_n) - h, & x_n \geq x_{\text{th}}, \end{cases} \tag{2.7}$$

where [2] considered specifically the Beverton–Holt map for f and x_{th} is a threshold population size. The difference from (2.3) is that TCC compares the threshold with the population size $f(x_n)$ *after* reproduction, whereas (2.7) compares the threshold with the population size x_n *before* reproduction. However, for the monotone population maps considered in this paper, there is a correspondence between (2.3) and (2.7). To see this, we note that f is bijective and that we just have to establish the following relation: $T := f(x_{\text{th}})$, $H := h$ or, equivalently, $x_{\text{th}} := f^{-1}(T)$, $h := H$ for $T \in (0, K)$, $H \in (0, T)$. The correspondence allows us to use some results obtained in [2] on the existence of (stable or unstable) 2-cycles and describe the bifurcations of F^2 (see subsection 5.3). For nonmonotone population maps like the Ricker map, there can be two break points in the harvest rule (2.3), and there is no correspondence between (2.3) and (2.7). That is, the two harvest strategies could differ qualitatively in their dynamics. As the harvest rule in (2.7) refers to a measurement of population size that is further in the past, this introduces a time lag that, for overcompensatory population maps, could lead to delayed density-dependent effects which are known to change dynamics quantitatively and qualitatively [34, 27, 17].

Second, TCC corresponds to a special case of a harvest control rule considered in [30]. This reference tested the strategy with simulations of a model specific for Baltic Sea cod. It found that the long-term yield was almost not affected by fishery closures due to the threshold, at least for the catch levels and thresholds they considered.

Third, [40] studied a special case of TCC, called the *precautionary threshold constant-catch (PTCC)*. This reference assumed that at least a minimum stock greater than the threshold must remain after harvesting. This constraint removes the discontinuity at the threshold point. We will see that the dynamics and bifurcation sequences in TCC are considerably richer than in PTCC. This illustrates the relevance of accounting for discontinuities in harvest control rules.

3. Background for piecewise-smooth maps. For the sake of completeness, this section defines some notions used throughout the paper. In subsection 3.1, we start by recalling some stability concepts: absorbing set; attracting and repelling set; stable, semistable, and unstable fixed points; etc. (for further reference, see Chapter 1 in [3]). In subsection 3.2, we will then establish some terms related to bifurcations in piecewise-smooth maps, such as break points and border-collision bifurcations. We follow the terminology in [3, 13]; see also [40].

Readers familiar with the terminology of nonsmooth dynamical systems may want to skip this section entirely. Readers familiar with smooth but not with nonsmooth dynamical

systems may want to jump to subsection 3.2.

3.1. Stability concepts. Let us consider a piecewise-smooth map $h : J \longrightarrow J$, where $J \subset \mathbb{R}$ is an interval.

A *critical point* c is a local extremum associated with the continuous branches of h or a limiting value of the function h at the discontinuity points. A set $E \subset J$ is *absorbing* if $h(E) \subseteq E$ (either E is invariant, $h(E) = E$; or it is strictly mapped into itself, $h(E) \subsetneq E$); there exists a neighborhood $\mathcal{U}$ of E such that any point in $\mathcal{U}$ is mapped inside E in a finite number of iterations; E is bounded by two different critical points, or a critical point and its image.

A closed invariant set R is called *repelling* if there exists a neighborhood $\mathcal{U}$ of R such that every point in $\mathcal{U}\backslash R$ is mapped outside $\mathcal{U}$ in a finite number of iterations. An *attracting set* $A \subset J$ is a closed invariant set for which there exists a neighborhood $\mathcal{U}$ of A such that $h(\mathcal{U}) \subset \mathcal{U}$ and $\cap_{i=0}^{\infty} h^i(\mathcal{U}) = A$. An *attractor* $\mathcal{A}$ is an attracting set with a dense orbit. Discontinuous one-dimensional maps can have four types of attractors: k-cycles and k-band chaotic attractors, $k \geq 1$; and two other types of attractors associated with quasi-periodic orbits. In general, we use the notation *oscillatory attractor* for those attractors which are not fixed points of the map h.

For a fixed point $x^* \in J$, defined by $h(x^*) = x^*$, we use some additional notions. First, a repelling fixed point is also called *unstable*. The fixed point x^* is *stable* if for all neighborhoods V of x^*, there exists another neighborhood U of x^* such that $h^n(x) \in V$ for all $x \in U$, $n \geq 1$. We say x^* is *locally asymptotically stable* (LAS) if it is stable and an attractor. If x^* is an attractor with $\mathcal{U} = J$, we say that x^* is a *global attractor*. If a global attractor is stable, then we refer to it as *globally asymptotically stable* (GAS). If x^* is not an attractor, but $\lim_{n\to\infty} h(x) = x^*$ for all $x \in [x^*, x^* + \varepsilon)$ or $x \in (x^* + \varepsilon, x^*]$ and some $\varepsilon > 0$, then we say x^* is *semistable*. Besides, if x^* is not an attractor but $\lim_{n\to\infty} h^n(x) = x^*$ for Lebesgue almost all x in a neighborhood $\mathcal{U}$ of x^*, we say that x^* is an *essential attractor*; if $\mathcal{U} = J$, then we call x^* an *essential global attractor*.

3.2. Bifurcation types. The notion of a bifurcation is associated with a qualitative change in the system dynamics under infinitesimal variation of parameters. Generally, we study bifurcations of attractors, but bifurcations of other invariant sets are also worth being investigated since they can influence the asymptotic dynamics as well. In the piecewise-smooth one-dimensional system (2.3), we find different types of bifurcations: smooth bifurcations (SBs), border-collision bifurcations (BCBs), basin boundary metamorphoses, and boundary-collision bifurcations.

We use the term *smooth bifurcations* for those bifurcations typical of smooth dynamical systems, which are associated with the eigenvalues of a fixed point or a cycle passing through the values ± 1. For piecewise-smooth maps, they can occur under some degeneracy conditions; in this case, we refer to them as *degenerate SBs*. We use the term *nonsmooth bifurcation* for those bifurcations which do not belong to any one of these types.

The points where F is not differentiable are called *break points*. If a break point is a fixed point of F, then we say it is a *boundary fixed point*. We recall that the map F in (2.4) is defined by two (if $H < T$) or three (if $H \geq T$) differentiable maps: f, g, and the constant map 0. There are fixed points of f or g that are not fixed points of F; we refer to them as

virtual fixed points. The fixed points of F are called *admissible fixed points*.

Border-collision bifurcations of fixed points occur when, under infinitesimal parameter variation, a fixed point collides with a break point and the collision leads to a qualitative change in the dynamics, with the fixed point transitioning from being admissible to being virtual or vice versa. Analogous definitions can be provided for k-cycles considering the map F^k instead of F, where F^k denotes k iterations of F.

A different group of bifurcations are related to abrupt changes in the basins of attraction, frequently referred to as *basin boundary metamorphoses* [23]. We will find transitions from a simply connected to a multiply connected basin as a parameter is being varied, but note that more complex transitions have been reported for other systems, e.g., from smooth to fractal basin boundaries [23].

Finally, *boundary-collision bifurcations* are caused by the collision of an attractor with an unstable k-cycle or fixed point. These bifurcations were introduced as crises in [22] for the case of a chaotic attractor. The bifurcation is called a *boundary crisis* when the unstable orbit is on the boundary of the chaotic attractor and the collision destroys the chaotic attractor. The bifurcation is called an *interior crisis* when the collision occurs within the basin of attraction. An interior crisis often results in a sudden expansion of the basin of attraction.

4. Equilibria, stability, and absorbing intervals. A key characteristic of the CC rule is its propensity to drive populations extinct. Even for small and moderate values of the maximum allowed quota H, $H \leq H_{20}$, the population can go extinct if the initial population size is small (see subsection 2.2). For large harvesting pressures, $H > H_{20}$, extinction is guaranteed for all initial conditions. The maximum sustainable yield that can be obtained with CC corresponds exactly to the critical quota level at the brink of guaranteed extinction. Harvesting at the MSY is therefore particularly risky.

One of the main results for TCC is that it can avoid the extinction risk imminent in CC. If the harvest control parameters are chosen such that $H < T$, then population survival is guaranteed for all initial conditions. This is because assumption **(A)** ensures that $F(x) > 0$ for all $x > 0$ and $F'(0_+) > 1$; thus, all positive initial conditions avoid extinction. In addition, if $T \leq K$, then, after a finite number of generations, all initial conditions remain in $[T-H, T]$, with $T - H > 0$; we call this scenario *population persistence* or simply *persistence*.

In the following, we study in detail the dynamics of the TCC rule governed by (2.3), when $0 < T < \sup\{f(x),\ x > 0\}$ and $H > 0$. We provide theoretical results on the stability of fixed points and the existence of absorbing intervals. The proofs are provided in Appendix A.1.

We begin by considering the case when the map F has a positive attractor or semistable equilibrium. An interpretation of some critical quota values can be found in Figures 3 and 5. In the following, for $T < H < \sup\{f(x) : x > 0\}$, let $m = \inf\{x > 0 : F(x) = 0\}$ and $M = \sup\{x > 0 : F(x) = 0\}$.

Proposition 4.1. *Assume that f satisfies* **(A)**. *Denote by x^*_- and x^*_+, when they exist, the positive fixed points of $g(x) = f(x) - H$, with $0 < x^*_- \leq \tilde{x} \leq x^*_- < K$. Then the following hold:*

(i) *If $T > K$, then K is the unique positive equilibrium. K is GAS for $H < T$. For $T \leq H$, K is LAS with the basin of attraction $(0, m) \cup (M, \infty)$, and all initial conditions in $[m, M]$ converge to 0.*

(ii) *If* $f(\tilde{x}) \le T < K$ *and* $H \le H_{10} = T - \widetilde{x_+^*}$, *where* $f\left(\widetilde{x_+^*}\right) = T$, *then* $x_+^* \in \left[\widetilde{x_+^*}, K\right)$ *is the unique positive fixed point; it is GAS if* $H < H_{10}$ *and a global attractor if* $H = H_{10}$.

(iii) *If* $0 < T < f(\tilde{x})$, *then the following hold:*

(a) *If* $H < H_{12} = T - \widetilde{x_-^*}$, *where* $f\left(\widetilde{x_-^*}\right) = T$, *then* $x_+^* \in [\tilde{x}, K)$ *is the unique positive fixed point and it is GAS.*

(b) *If* $H_{12} \le H < H_{20} = f(\tilde{x}) - \tilde{x}$, *then* $x_-^* < \tilde{x}$ *is unstable for all* $H \ne H_{oscill} = f(T) - T$ *and* $x_+^* > \tilde{x}$ *is LAS with* (x_-^*, ∞) *contained in its basin of attraction. In particular, if* $0 < T < \tilde{x}$ *and* $H_{oscill} \le H < H_{20}$, *then* x_+^* *is LAS and it attracts exactly* (x_-^*, ∞).

(c) *If* $H = H_{20}$, *then* $\tilde{x}$ *is the unique positive fixed point; it is at least semistable, and* $[\tilde{x}, \infty)$ *belongs to its basin of attraction.*

Now, we focus our attention on the cases where there is an absorbing interval which does not contain any positive attractor or semistable equilibrium.

Proposition 4.2. *Assume that* f *satisfies* **(A)** *and that* $T \le K$. *Denote by* x_-^* *and* x_+^*, *when they exist, the positive fixed points of* $g(x) = f(x) - H$, *with* $0 < x_-^* \le \tilde{x} \le x_-^* < K$. *If any of the following conditions hold, then the interval* $I = [\max\{0, T - H\}, T]$ *is absorbing and does not contain any positive fixed point:*

(a) $T = K$, $H > 0$.
(b) $f(\tilde{x}) \le T < K$, $H > H_{10}$.
(c) $0 < T < f(\tilde{x})$, $H > H_{20}$.
(d) $0 < T < \tilde{x}$, $H \in (H_{oscill}, H_{20})$.

In cases (a), (b), *and* (c), *all orbits of* (2.3) *enter the interval* I *in finite time. In case* (d), *orbits starting at* $x_0 \in (0, x_-^*)$ *enter* I *after a finite number of generations, but the positive fixed point* $x_+^* > T$ *attracts* (x_-^*, ∞).

In view of Propositions 4.1 and 4.2, there are different regions in the control parameter plane (H, T) where the long-term behavior of the solutions of (2.3) depends on the initial condition. This will be investigated in more detail in the following sections.

5. Bifurcations.

For the TCC rule (2.3) and a population map f satisfying condition **(A)**, F is a piecewise-smooth discontinuous map. It is therefore interesting to analyze the possible bifurcations, using as bifurcation parameters the control variables H and T. We begin by dealing with fixed point BCBs or SBs and basin boundary metamorphoses for a general map f. Then, for the particular case of the Beverton–Holt model, we determine 2-cycle BCBs or SBs and boundary-collision bifurcations. For nonsmooth bifurcations, we first give a general description of the associated long-term dynamics; then we determine the parameter values at which the bifurcation takes place, and we provide a more detailed description of the corresponding asymptotic dynamics. It is also worth mentioning that most of this information comes from analytical results in section 4, [13, section 4.2], and [2, section 4]. Therefore, it is clearly indicated if the dynamical behavior is deduced from numerical one-parameter bifurcation diagrams, that is, from simulations.

5.1. Fixed point BCBs and SBs.

In the following, we describe the possible dynamical scenarios at a BCB defined by a boundary fixed point. See Figure 3 for illustrations:

- An *existence BCB* occurs when a virtual fixed point of F becomes admissible. If the

new admissible equilibrium is unstable, there is a transition from (global) attraction to essential (global) attraction in the dynamics; while if the new admissible fixed point is stable, then there is a transition from convergence of all initial conditions (ICs) to another fixed point to some sort of bistability between both equilibria. This bifurcation takes place when the following hold:

  - $0 < T < f(\tilde{x})$, $H = H_{12}$: By Proposition 4.1, we know that the unstable fixed point x_-^* of g becomes admissible and the GAS fixed point x_+^* becomes LAS (in fact, bifurcation diagrams suggest that x_+^* becomes an essential global attractor) when H is increased or T is decreased. See Figure 3(A1)–(A3).
  - $T = K$, $H > T$: By Proposition 4.1, we know that the stable fixed point K of f becomes an admissible fixed point and there is a transition as T is increased from all ICs converging to the unstable equilibrium 0 (observed in one-parameter bifurcation diagrams) to a bistable scenario in which ICs in $[m, M]$ converge to 0 and ICs in $[0, \infty)\backslash[m, M]$ converge to the LAS fixed point K.

- A *period-adding BCB* occurs when an LAS admissible fixed point collides with a break point. At the collision point, there is a homoclinic orbit; after the collision, the fixed point becomes virtual, and an attracting m-periodic orbit becomes admissible, giving rise to a *period-adding scenario* (for details, see Chapter 3 in [3]). This bifurcation takes place when the following hold:
  - $f(\tilde{x}) < T < K$, $H = H_{10}$: For $H < H_{10}$, by Proposition 4.1 we know that the admissible fixed point x_+^*, with $g'(x_+^*) \in (0, 1)$, is GAS in $(0, \infty)$. At $H = H_{10}$, the equilibrium x_+^* collides with a break point; from the results in subsection 4.2.3 in [13], we deduce that, as H or T are increased, an attracting long-period cycle becomes admissible. See Figure 3(B1)–(B3).
  - $T = K$, $H < T$: For $T > K$, by Proposition 4.1 we know that the admissible equilibrium K is GAS in $(0, \infty)$. At $T = K$, the virtual fixed point K, with $f'(K) \in (0, 1)$, collides with a break point; from the results in subsection 4.2.3 in [13], we deduce that, as T is decreased, an attracting long-period cycle becomes admissible.

There is also a fold SB when $0 < T < f(\tilde{x})$, $H = H_{20}$: The admissible fixed points $x_-^* \leq \tilde{x} \leq x_+^*$ of g collide and suddenly disappear when H is increased. This fold SB also exists in the CC rule and is "inherited" by TCC.

Figure 6 is a two-parameter bifurcation diagram for the case where f is the Beverton–Holt map. In this diagram, we represent fixed point BCBs and SBs for F with solid and dashed curves, respectively. Dark blue is for existence BCBs, magenta for period-adding BCBs, and red for fold SB.

5.2. Basin boundary metamorphoses. These types of bifurcations occur when there is a transition from coexistence of an (essential) global attractor $\mathcal{A}$ and an admissible repelling fixed point $\mathcal{R}$ of F to some sort of bistability between the attractor $\mathcal{A}$ and $\mathcal{R}$, in such a way that $\mathcal{R}$ is still repelling but some ICs converge to it. These bifurcations take place when the following hold:

- $0 < T < H_{20} = f(\tilde{x}) - \tilde{x}$, $H = T < H_{\text{oscill}}$: 0 is an admissible unstable equilibrium, and bifurcation diagrams suggest that x_+^* is an essential global attractor for all $0 < H < T$.

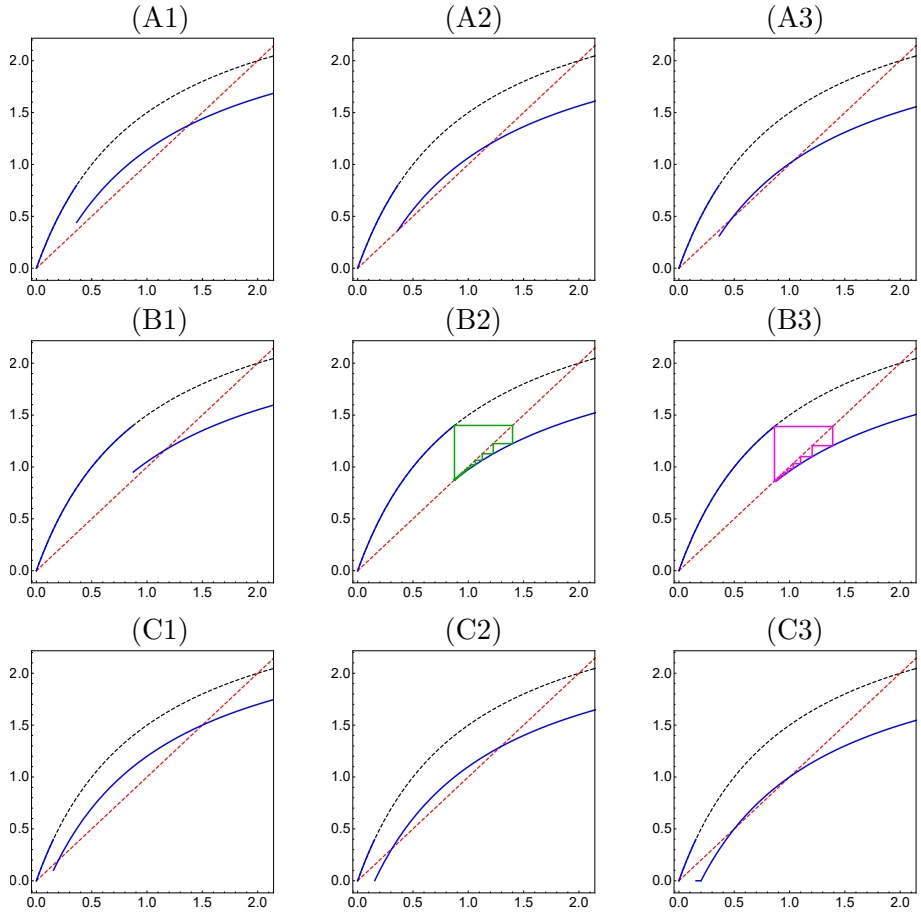

Figure 3. *Illustrations of fixed point BCBs and basin boundary metamorphoses arising in the TCC rule (2.3). The Beverton–Holt map $f(x) = 3x/(1+x)$ is the black dashed curve, and the blue solid curve is the corresponding map F. The red dashed line is $y = x$. The attracting cycles $\{x_0, F(x_0), F^2(x_0), \ldots\}$ and homoclinic orbits are shown in magenta and green, respectively.* Top panels: *Existence BCB for $T = 0.8 < f(\tilde{x}) \approx 1.27$.* (A1)*: $H = 0.36 < H_{12} \approx 0.44$;* (A2)*: $H = H_{12}$;* (A3)*: $H = 0.49 > H_{12}$.* Mid-panels: *Period-adding BCB for $f(\tilde{x}) < T = 1.4 < K = 2$.* (B1)*: $H = 0.45 < H_{10} \approx 0.53$;* (B2)*: $H = H_{10}$, homoclinic orbit;* (B3)*: $H = 0.54 > H_{10}$, $F^9(x_0) = x_0$.* Bottom panels: *Basin boundary metamorphosis for $0 < T = 0.4 < \min\{H_{20}, H_{oscill}\} \approx 0.46$.* (C1)*: $H = 0.3 < T$;* (C2)*: $H = 0.4 = T$;* (C3)*: $H = 0.45 \in (H_{oscill}, T)$.*

As H is increased or T is decreased through $H = T$, x_+^* is LAS and the fixed point 0 is still unstable but the ICs in $[m, M]$ converge to it. See Figure 3(C1)–(C3).

- $T > K$, $H = T$: By Proposition 4.1, we know that K is GAS in $(0, \infty)$ and 0 is unstable for all $0 < H < T$. As H is increased or T is decreased through $H = T$, K becomes LAS and 0 is still repelling but the ICs in $[m, M]$ converge to it.

In Figure 6, basin boundary metamorphoses are shown as orange solid lines.

5.3. 2-cycle BCBs and SBs.

2-cycle BCBs are fixed point BCBs of the piecewise-smooth map $F^2 = F \circ F$. Here, we can classify them in the light of Theorem 4.4 in [2] for the TCC rule with $f(x) = r\,x/(1+x)$, $r > 1$.

We focus our attention on the region of the parameter plane (H, T) where $H < T < K$. This is because numerical simulations suggest that for $H \geq T$ there might be oscillations in addition to the fixed points, but these oscillations could be complex attractors or long transients that eventually result in extinction.

At the outset, we fix some notations for relevant values of the harvesting parameters H and T. We define $H^* := (r-1)^2/(r+1)$, which is determined as the solution of the nonlinear system $f(g(x)) = x$, $f'(g(x))g'(x) = 1$. And we define $T^* > 0$ as the unique solution of the nonlinear equation $g \circ f(T^* - H^*) = T^* - H^*$, with $g(x) = f(x) - H^*$. The BCBs for F^2 are determined by $F^2(T-H) = g \circ f(T-H) = T - H$ (with $F(T-H) \neq T-H$) or by $F^2(T) = f \circ g(T) = T$ (with $F(T) \neq T$).

We distinguish the following three cases:

- For $0 < T < T^*$ and $g \circ f(T-H) = T - H$, the unstable equilibrium of $g \circ f$ becomes admissible as H is increased or T continuously changes through an existence BCB for F^2. Then, the stable and unstable 2-cycles coexist and bifurcation diagrams suggest that the stable 2-cycle is an essential global attractor.
- For $T^* < T < K$ and $g \circ f(T-H) = T - H$, the admissible stable fixed point of $g \circ f$ collides with a break point of F^2. At the collision point, there is a homoclinic orbit; after the collision, an attracting l-periodic cycle of F becomes admissible, as T or H are increased, through a period-adding BCB for F^2.We apply the results of subsection 4.2.3 in [13] to the map F^2 that satisfies $(F^2)'(T-H) \in (0,1)$ for all $T \in (T^*, K)$, $H \in (0, H^*)$ such that $g \circ f(T-H) = T - H$.
- For $H^* < T < K$ and $f \circ g(T) = T$, the stable fixed point of $f \circ g$ collides with a break point of F^2 and becomes admissible as H or T are increased in a variety of BCBs. Again, we can apply the results of subsection 4.2.3 in [13] to the map F^2 when $f(\tilde{x}) < T < K$. Thus, if $(F^2)'(T-H) \in (0,1)$ at the bifurcation point, then we have a period-adding BCB (see Figure 4); otherwise, we expect more complex bifurcations. However, for $H^* < T < f(\tilde{x})$, the presence of the unstable 2-cycle influences the asymptotic dynamics and the one-parameter bifurcation diagram in Figure 8(C) suggests that the bifurcations are more complex.

The coexisting 2-cycles (stable and unstable fixed points of $f \circ g$) are destroyed when a fold SB for F^2 occurs at H^*.

In Figure 6, existence BCBs of 2-cycles are shown in the light blue solid line, period-adding and more complex BCBs of 2-cycles in the purple solid line, and fold SBs of 2-cycles in the dotted red line.

5.4. Boundary-collision bifurcations. When applying the TCC rule to such a simple map as $f(x) = r\,x/(1+x)$, $r > 1$, the asymptotic population dynamics can also change through a boundary-collision bifurcation, in which an oscillatory attractor, which is contained in the absorbing interval $I = [\max\{0, T-H\}, T]$, reaches the break points T or 0 and collides with an unstable equilibrium, x^*_- or 0. Subsection 1.8.3 in [3] mentions that the boundaries of chaotic attractors of one-dimensional maps are determined by critical points, i.e., local extrema and break points, and their images. These types of bifurcation take place when the following hold:

- $0 < T < \tilde{x}$, $H = H_{\text{oscill}} < T$: For all $H_{\text{oscill}} < H < \min\{T, H_{20}\}$, $I = [T-H, T]$ is an absorbing interval, such that all ICs in $(0, x^*_-)$ enter I in finite time. Moreover, for all

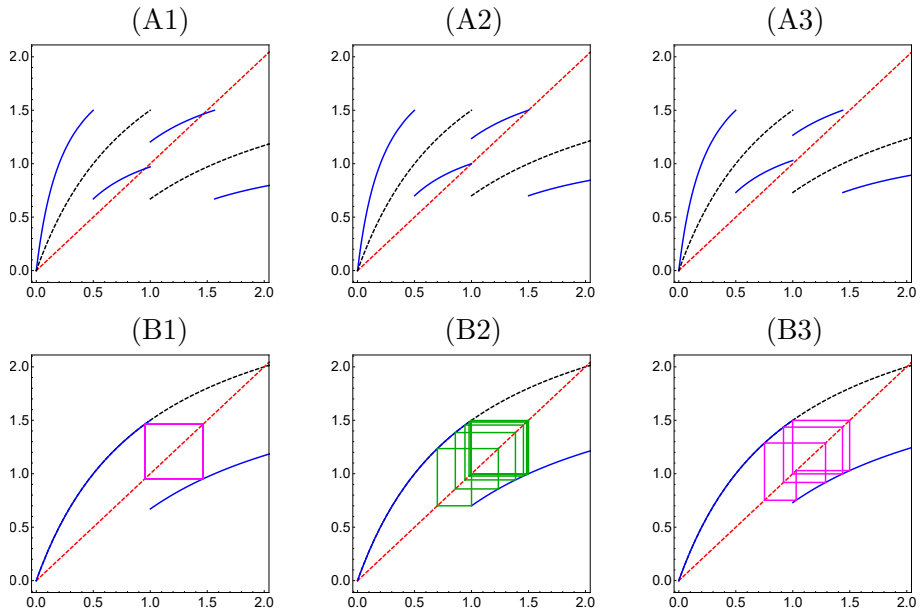

Figure 4. *Illustration of a* 2*-cycle BCB. Panels in the* top row *show* F *as a black dashed curve and* F^2 *as a blue solid curve. Panels in the* bottom row *show* f *as a black dashed curve and* F *as a blue solid curve. In all panels, the red dashed line is* $y = x$*, and the TCC rule* (2.3) *is applied to the Beverton–Holt map* $f(x) = 3x/(1+x)$ *with* $f(\tilde{x}) \approx 1.27 < T = T^* = 1.5 < K = 2$*. Across the columns, parameter* H *is decreased, giving rise to a homoclinic orbit and several period-adding BCBs.* (Left) $H = 0.83$*, with the magenta box in panel* (B1) *representing an attracting* 2*-cycle.* (Middle) $H = 0.8$ *such that* $F^2(T) = f(f(T) - H) = T$*, with a homoclinic orbit shown in green in panel* (B2)*; it appears when the attracting* 2*-cycle collides with a break point of* F^2 *in a period-adding BCB.* (Right) $H = 0.77$*, with an attracting* 7*-periodic orbit shown in magenta.*

$x_0 \in I$ and $n \in \mathbb{N}$, $(F^n)'(x_0) > 1$, consequently all n-cycles contained in I are unstable and the oscillatory attractor contained in I is chaotic, so it collides with $T = x^*_-$ at $H = H_{\text{oscill}}$. Then, as H is decreased or T is increased, bifurcation diagrams suggest that x^*_+ becomes an essential global attractor. See Figure 5 for an illustration.

- $0 < T < \tilde{x}$, $H = T \in (H_{\text{oscill}}, H_{20})$ or $0 < T < f(\tilde{x})$, $H = T > H_{20}$ or $f(\tilde{x}) \le T < K$, $H = T = H_{10}$: For values of the harvesting quota H slightly smaller than T, the absorbing interval $I = [T - H, T]$ contains an oscillatory attractor, and the ICs in either $(0, x^*_-)$ or $(0, \infty)$ enter I in finite time. At $H = T$, if the attractor in I is chaotic, it collides with $T - H = 0$; and, as H is increased or T is decreased, at least some positive ICs in I converge to the unstable fixed point 0.
  For $0 < T < f(\tilde{x})$, $H = T > H_{20}$ or $f(\tilde{x}) \le T < K$, $H = T = H_{10}$, bifurcation diagrams suggest that, as H is increased or T is decreased through $H = T$, either there is some sort of bistability between an oscillatory attractor and the unstable equilibrium 0, or all ICs converge to 0 but there exist long transients (see Figure 8(A)).

In Figure 6, boundary-collision bifurcations are shown in the solid black line.

6. Impact of T and H on population dynamics. In this section, we present bifurcation diagrams to better understand the role played by the harvesting parameters H and T in the population dynamics of the TCC rule (2.3).

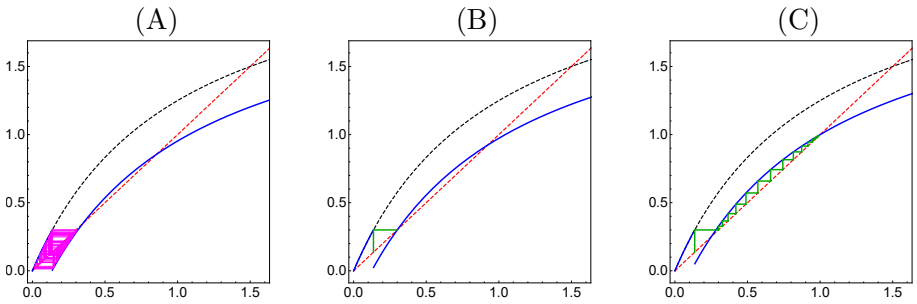

Figure 5. *Illustration of a boundary-collision bifurcation for decreasing harvest quotas H in the TCC rule with the Beverton–Holt map $f(x) = 2.5\,x/(1+x)$ and $T = 0.3 < \tilde{x} \approx 0.58$. The red dashed line is $y = x$. We represent the orbit of x_T such that $f(x_T) = T$ in magenta or green if it converges to an oscillatory attractor or an equilibrium, respectively.* (A) *$H_{oscill} \approx 0.28 < H = 0.3 < T$ such that there is an oscillatory attractor contained in $I = [T - H, T]$.* (B) *$H = H_{oscill}$ such that the oscillatory attractor collides with the fixed point $T = x^*_-$.* (C) *$H = 0.25 < H_{oscill}$ such that, as $f(x_T) = T > x^*_-$, the point $x_T < x^*_-$ belongs to the basin of attraction of the LAS equilibrium x^*_+.*

We first plot a two-parameter bifurcation diagram which gives a global picture of the dynamics in terms of both harvest control parameters. Then, we study some one-parameter bifurcation diagrams, which help us to understand some features of the dynamics. We will observe several dynamical regimes, which are indicated with a certain color code in the two-parameter bifurcation diagram. To facilitate visual orientation, the same color code is used in the background of the one-parameter bifurcation diagrams to match the dynamical regimes.

6.1. Dynamical regimes. The two-parameter bifurcation diagram in Figure 6 gives a detailed description of the dynamics and bifurcations of the TCC rule (2.3) with the Beverton–Holt map $f(x) = 3\,x/(1+x)$, in terms of the relevant control parameters H and T. The bifurcation diagram has been obtained by using the implicit or explicit analytic expressions previously described in sections 4 and 5. However, we emphasize that, in some particular cases, the determination of the type of bifurcation is conjectured by using information from numerical one-parameter bifurcation diagrams; see section 5 for details.

For a general population map f satisfying condition **(A)**, we define and identify the following dynamical regimes, which exist in certain parameter regions. They are marked with different colors in the two-parameter bifurcation diagram of Figure 6 and the one-parameter bifurcation diagrams of Figures 7 to 9. For each dynamical regime, we additionally describe what the dynamics of CC would look like (cf. Proposition 2.1) and what effect TCC has in comparison to CC. It is worth mentioning that we use the statements about the asymptotic dynamics of TCC described in sections 4 and 5; as a consequence, some assertions might come from evidence observed in numerical one-parameter bifurcation diagrams, e.g., when we assert that a fixed point is an essential global attractor.

- *Unconditional persistence* (light blue): TCC guarantees persistence and convergence to an equilibrium for all initial conditions. This dynamical regime is not possible for the CC rule with $H > 0$ and $T = 0$. In comparison to CC, TCC allows for unconditional persistence in the following ways:
  - Bistability between extinction and the LAS equilibrium $x^*_+ > \tilde{x}$ in CC is replaced

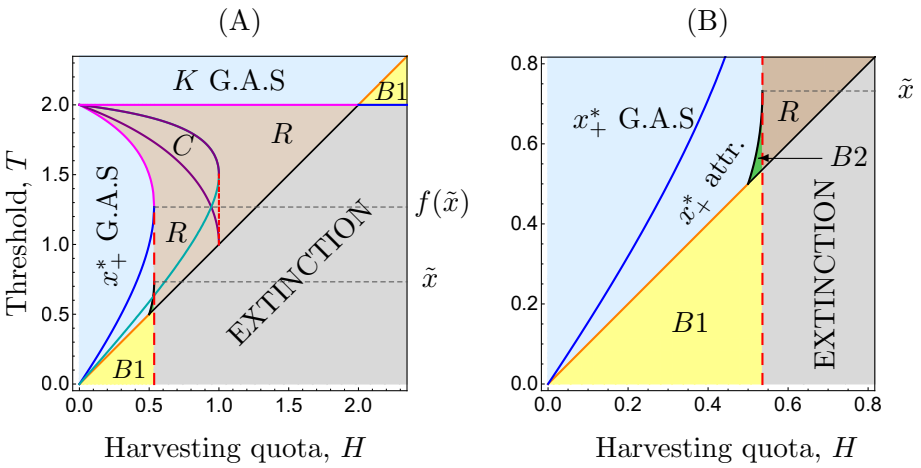

Figure 6. (A) *Main bifurcation curves of TCC with the Beverton–Holt map* $f(x) = 3x/(1+x)$ *in the two-parameter plane of the harvest control variables. Solid lines are for bifurcations involving break points, that is, BCBs, basin boundary metamorphoses, and boundary-collision bifurcations. Dashed and dotted lines are for smooth bifurcations (SBs) of* F *and* F^2*, respectively. Bifurcations of fixed points are shown in dark blue for existence BCBs, magenta for period-adding BCBs, and red for fold SBs. Bifurcations of* 2*-cycles are shown in light blue for existence BCBs, purple for period-adding or more complex BCBs, and red for fold SBs. Basin boundary metamorphoses are shown in orange and boundary-collision bifurcations in black. Parameter regions labeled with* $B1$ *exhibit either bistability between the unstable fixed point* 0 *and another LAS equilibrium* (x_+^* *or* K*) or tristability if there exists an oscillatory attractor instead of long transients. Complex behavior (*m*-cycles with* $m > 3$ *or chaos) may be expected in regions marked with* R*. The region labeled with* C *has an attracting* 2*-cycle. In the region labeled with EXTINCTION, there may exist long transients for some ICs ending in extinction or bistability between* 0 *and an oscillatory attractor. Colored areas indicate dynamical regimes that are explained in the main text.* (B) *Enlargement of* (*A*) *for* $0 < T < \tilde{x}$*. The region labeled with* $B2$ *exhibits bistability between the LAS equilibrium* x_+^* *and an oscillatory attractor (*m*-periodic with* $m > 3$ *or chaotic), contained in the absorbing interval* $I = [T - H, T]$*.*

by the (essential) global attractor x_+^* or K. This dynamics takes place when the following hold: $0 < T < f(\tilde{x})$, $0 < H < \min\{T, H_{\text{oscill}}, H_{20}\}$ (see the top panel in Figure 3 and Figure 5(C)); $f(\tilde{x}) \le T < K$, $0 < H < H_{10}$ (see Figure 3(C1)); and $K < T < \sup\{f(x) : x > 0\}$, $H < H_{20}$.

- Extinction in CC is replaced by global attraction to K, when $K < T < \sup\{f(x) : x > 0\}$ and $H_{20} < H < T$.

- *Conditional persistence* (yellow): Some initial conditions lead to population persistence, whereas other initial conditions lead to extinction. In comparison with CC, TCC reduces the set of ICs which converge to 0 in several ways:
  - If $0 < T < f(\tilde{x})$ and $T \le H < H_{\text{oscill}} < H_{20}$, then $T > x_-^*$ and some ICs in $(0, x_-^*)$ converge to the LAS equilibrium x_+^* instead of being led to extinction.
  - If $0 < T < f(\tilde{x})$ and $\max\{H_{\text{oscill}}, T\} < H < H_{20}$, then $T < x_-^*$ and the interval $I = [0, T]$ is absorbing. Numerical bifurcation diagrams suggest that some ICs in $(0, x_-^*)$ converge to 0 but other ICs in $(0, x_-^*)$ may oscillate in I, at least during long periods of time before being led to extinction (see Figure 7(A)). All ICs in (x_-^*, ∞) converge to x_+^* as in the CC rule.

  - If $K < T < \sup\{f(x) : x > 0\}$ and $T < H$, then all ICs in $(0, K]$ converge to the LAS equilibrium K instead of being led to extinction.
- *Unconditional oscillatory persistence of small populations* (green): TCC guarantees persistence for all ICs; there is bistability between x_+^* and an oscillatory attractor. The latter attracts small population sizes. More specifically, all ICs in $(0, x_-^*)$ remain oscillating in $[T - H, T] \subset (0, x_-^*)$ instead of being led to extinction in the case of CC. This situation takes place when $0 < T < \tilde{x}$ and $H_{\text{oscill}} < H < \min\{H_{20}, T\}$ (see Figure 5(A)).
- *Unconditional oscillatory persistence of all ICs* (brown): TCC guarantees persistence in the form of oscillatory attractors for all ICs. This dynamical regime does not exist in CC and occurs in TCC in the following ways:
  - If $0 < T < K$ and $H_{20} < H < T$, then extinction in CC is replaced by persistence in the interval $I = [T - H, T]$ for all ICs.
  - If $f(\tilde{x}) < T < K$ and $H_{10} < H < H_{20}$, then bistability between the LAS equilibria x_+^* and 0 is replaced by persistence in $I = [T - H, T]$ for all ICs.
- *Extinction* (grey): All ICs eventually go extinct. This occurs in TCC if $0 < T < K$ and $H > \max\{T, H_{20}\}$. Numerical bifurcation diagrams suggest that either all ICs lead quickly to extinction or that some positive ICs converge to 0 while others may oscillate in $I = (0, T]$, at least during long periods of time before being led to extinction. The dynamical regime of extinction for all ICs also exists in CC, but the possibility that some ICs lead to long oscillations before eventual extinction is due to TCC.

We can summarize the main characteristics of Figure 6 by distinguishing the threshold value relative to the maximum allowed quota. On the one hand, in the case that $T > H$, the TCC strategy protects the population from extinction for all initial conditions. We can broadly distinguish three different variations. First, if $T > K$, there will be no harvesting, as the threshold is above the carrying capacity and K is GAS. Second, if $H < H_{20}$ and $\max\{\tilde{x}, H\} < T < f(\tilde{x})$, then x_+^* is an essential global attractor or GAS. Third, if $H > H_{20}$ so that the population would collapse under the CC rule, TCC guarantees persistence and there is an oscillatory attractor in the absorbing interval I for all $H < T < K = 2$.

On the other hand, in the case that $T < H$, the TCC strategy is not protective enough that it guarantees persistence for all initial conditions. Indeed, if $H > H_{20}$ such that extinction is inevitable under CC, this is also the case under TCC—unless $T > K$, in which case some initial conditions may persist. However, if $H < H_{20}$, CC leads to conditional persistence. TCC does not change this dynamical regime when $T < H$, but it makes extinction less likely because the set of initial conditions resulting in extinction is decreased.

In comparison with the PTCC strategy described in [40], we see that the discontinuity point of F in the TCC rule provokes a huge change in the dynamics. Recall that, for a population map f under condition **(A)**, the dynamics of PTCC are trivial in the sense that all solutions converge to an equilibrium.

6.2. One-parameter bifurcation diagrams. In the remainder of this section, we present some bifurcation scenarios that occur when varying one of the harvest control parameters. The bifurcation scenarios feature some typical bifurcation sequences occurring in piecewise-smooth discontinuous maps, according to a specific regularity, such as a *Farey tree* in a period-adding

scenario or a slightly modified *truncated skew tent map scenario*; a detailed explanation of both scenarios is given in Chapter 3 of [3]. If we consider other threshold and quota values, for instance $T = 1$ and $H \in (H_{20}, T)$, we observe other features, such as the *bandcount incrementing scenario*.

The bifurcation diagrams presented here have been obtained numerically in the following way for the TCC rule (2.3) with $f(x) = 3x/(1+x)$. For each value of a bifurcation parameter, we select a random initial condition from a suitable interval, and then we compute a number of iterations using the map F. After removing transients (600–700 iterations), we plot the remaining data (50–150 iterations) to get an idea of the asymptotic behavior. In the following one-parameter bifurcation diagrams, blue points/curves represent asymptotic population sizes. We recall that the background colors indicate the corresponding dynamical regimes previously described in subsection 6.1.

In the following subsections, we describe the asymptotic dynamics observed in the one-parameter bifurcation diagrams; some of them illustrate the ones previously determined in sections 4 and 5.

6.2.1. Varying the harvest quota H. Based on the two-parameter bifurcation analysis, it is obvious that the impact of varying H depends on the value of T. Here, we consider three different cases for T. We first deal with small values of T ($0 < T < \tilde{x}$), where we can expect oscillations resulting from TCC. We then consider large values of T ($f(\tilde{x}) < T < K$), where increased quota values H lead from an equilibrium being an (essential) global attractor to complex dynamics. Last, we consider intermediate values of T ($\tilde{x} < T < f(\tilde{x})$), where the bifurcation sequence is more complex than for small or large thresholds. When $\tilde{x} < T < K$, there is a transition from (essential) global attraction of x_+^* to periodic or complex dynamics; the transition is to periodic dynamics if $f'(T) = g'(T-H) < 1$ at the bifurcation point and it is to chaotic dynamics if $f'(T) = g'(T-H) > 1$ at the bifurcation point (see subsections 4.2.3 and 4.2.4 in [13]).

First, let us begin with a small threshold value, $T = 0.52 < \tilde{x} \approx 0.73$. As shown in Figure 7(A), there are five bifurcation points as H is increased from zero. For small to intermediate harvest quotas H, there is (essential) global attraction to the fixed point x_+^* of g (light blue background in Figure 7(A)). At the bifurcation value $H_3 = H_{\text{oscill}} \approx 0.51$, there is a boundary-collision bifurcation, creating bistability between the equilibrium x_+^* and an oscillatory attractor contained in $I = [T-H, T]$ (green background in Figure 7(A)). Their basins of attraction are separated by the unstable fixed point x_-^* of g. At $H_4 = T$, there is a boundary-collision bifurcation as the oscillatory attractor collides with the unstable fixed point 0; we then have a region of bistability between 0 and x_+^* (yellow background in Figure 7(A)). Notice that for quota values slightly greater than T, we observe oscillations which may be an oscillatory attractor or long transients; thus, there may be tristability between 0, x_+^*, and (long) oscillations. At $H_5 = H_{20} \approx 0.54$, a fold SB occurs and, for $H > H_5$, apparently, all ICs converge to 0 (grey background in Figure 7(A)). Furthermore, at $H_1 = H_{12} \approx 0.31$ and $H_2 \approx 0.45$ there are two existence BCBs for F and F^2, respectively; however, we do not plot the unstable 2-cycle in Figure 7(A) since it does not have much influence on the long-term dynamics.

Second, let us now consider a bifurcation sequence that occurs for large threshold values.

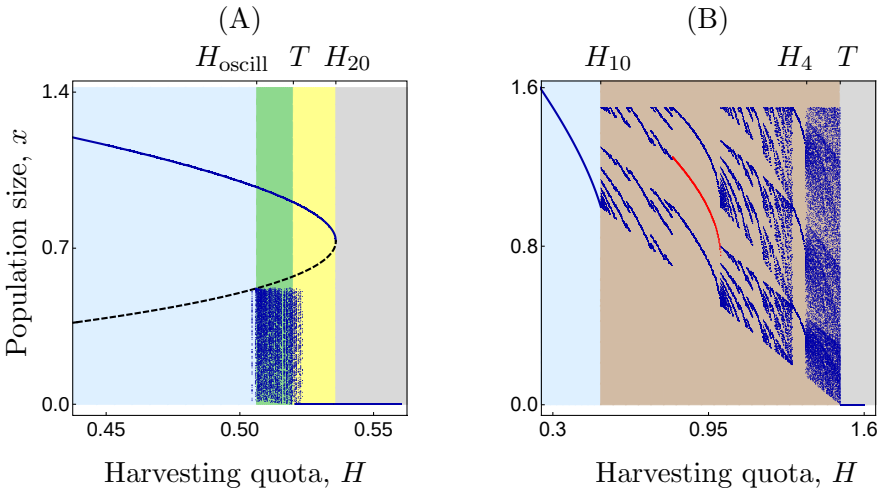

Figure 7. *Bifurcation sequences for increased harvest quotas H in the TCC rule (2.3).* (A) *Case for a small threshold value $T = 0.52 < \tilde{x} \approx 0.73$. The black dashed curve represents the unstable equilibrium x_-^* of g.* (B) *Case for a large threshold value $f(\tilde{x}) \approx 1.268 < T = T^* = 1.5 < K = 2$ and $H \in (0.3, 1.6)$. The red solid curve represents the average population size in the parameter region where the 2-cycle of $f \circ g$ is an attractor. Colored areas indicate dynamical regimes that are explained in subsection 6.1. See the main text for more details.*

This is illustrated in Figure 7(B) for $f(\tilde{x}) \approx 1.268 < T = T^* = 1.5 < K = 2$. At $H_1 = H_{10} \approx 0.5$, there is a period-adding BCB; and at $H_5 = T$, there is a BCB. In between these two bifurcations (brown background in Figure 7(B)), we observe oscillatory dynamics. As H is increased from H_{10} (where $f'(T) = g'(T - H) \in (0, 1)$), we find a period-adding scenario, also known as a *Farey tree*, where between two cycles of periods n and l there is an $(n + l)$-cycle. Between the period-adding BCBs at $H_2 \approx 0.8$ and $H_3 = H_* = 1$, there is an attracting 2-cycle. For some values of the quota $H \in (H_2, H_3)$, we see that the average population size is bigger than the GAS equilibrium x_+^* at $H_1 = H_{10}$; this means that an increased harvesting quota elevates the average population size, which is also known as the *hydra effect* [1, 27]. At $H_4 \approx 1.36$, there is a transition from an attracting 3-cycle to chaotic dynamics through a fold SB for $F^3 = f^2 \circ g$.

Third and last, we consider a bifurcation sequence that occurs for intermediate threshold values. This is illustrated in Figure 8(A) for $H^* = 1 < T = 1.1 < f(\tilde{x}) \approx 1.27$. As in Figure 7(B), we observe a region of oscillatory dynamics (brown background) between the two bifurcation points at $H_1 = H_{20} \approx 0.536$ (fold SB) and $H_4 = T$ (BCB). But now we find a different bifurcation sequence for this oscillatory parameter region. At $H_1 = H_{20}$, for increasing H there is a transition from the globally attracting fixed point $x_+^* < \tilde{x}$ to complex dynamics since $f'(T) = g'(T-H) > 1$ (Figure 8(A)). For even larger values of H, the complex dynamics are replaced by a period-adding scenario (Figure 8(B)). When further increasing H, we observe a sequence of bifurcations similar to those in a truncated skew tent map scenario, giving rise to an exchange between cyclic and more complex dynamics (Figure 8(C)–(D)). More precisely, at $H_3 = H^* = 1$ there is a fold SB for $F^2 = f \circ g$: as H is decreased, an unstable and a stable 2-cycle are created; then, at $H_2 \approx 0.992$, the stable 2-cycle becomes virtual, and

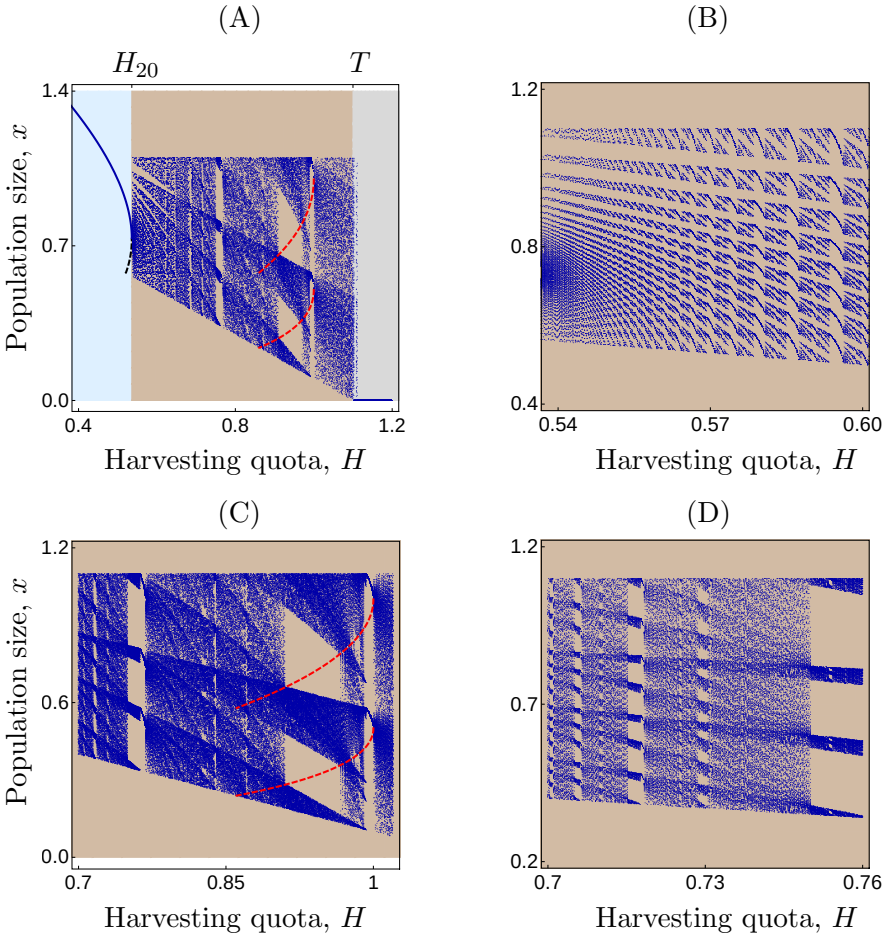

Figure 8. *Bifurcation sequence for an intermediate threshold value $T = 1.1 \in (H^*, f(\tilde{x})) \approx (1, 1.27)$ when increasing the harvest quota H in the TCC rule (2.3). The panels show repeated zooms into the bifurcation parameter H. The black dashed curve in* (A) *corresponds to the unstable fixed point x^*_- of g. The red dashed curves represent the unstable 2-cycle of $f \circ g$. Colored areas indicate dynamical regimes that are explained in subsection 6.1. See the main text for more details.*

after the BCB we observe complex dynamics. If we continue decreasing H (Figure 8(C)), the unstable orbit plays a role in the dynamics; between two collisions of the bands of the chaotic attractor with the unstable 2-cycle, the chaotic attractor does not fill the absorbing interval $I = [T - H, T]$. Note that the two boundary-collision bifurcations are interior crises.

6.2.2. Varying the harvest threshold T. Now we consider T as a bifurcation parameter while keeping the quota H fixed. Before doing so, we note that, according to the two-parameter bifurcation diagram in Figure 6, the dynamics are strongly influenced by the relative position of H with respect to the critical value H_{20}. Recall that this is the MSY under the CC rule and that it is shown as red dashed vertical line in Figure 6.

It is also worth mentioning that for $H < H_{20}$, a continuous variation (increasing or decreasing) of the threshold T can be either stabilizing or destabilizing (see Figure 9(A)).

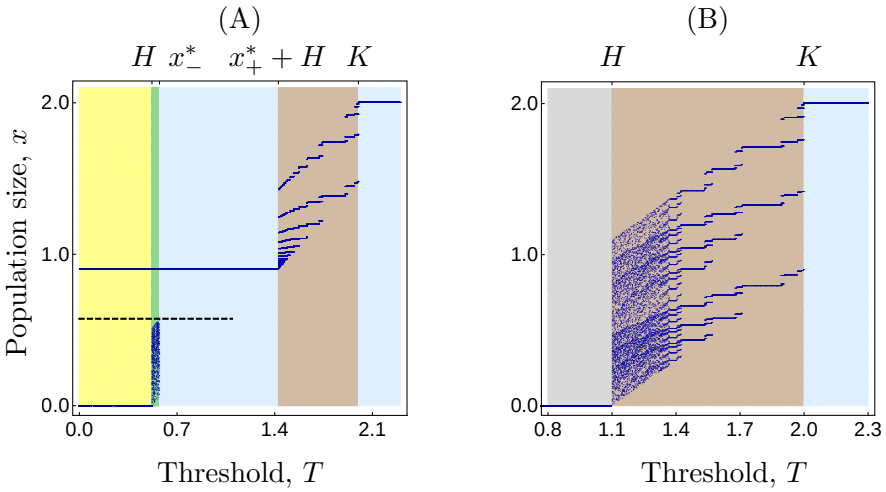

Figure 9. *Bifurcation sequences when varying the harvest threshold for the TCC rule (2.3).* (A)*: Case with modest harvest quota* $H = 0.52 < H_{20} \approx 0.54$. (B)*: Case with large harvest quota* $H = 1.1 > H^* = 1$. *We find a small region of transition from apparently chaos to a period-adding scenario. The black dashed curve in* (A) *corresponds to the unstable fixed point* x_-^* *of* g. *Colored areas indicate dynamical regimes that are explained in subsection 6.1. See the main text for more details.*

However, for $H > H_{20}$, an increment on the threshold T is always stabilizing (see Figure 9(B)), but the stable fixed point is the virgin stock K and exists for $T > K$, that is, for a very protective harvest rule that leads to no harvesting. By *stabilizing* we mean that an unstable equilibrium becomes locally stable. We use the term *destabilizing* when a stable fixed point loses its stability. Notice that for threshold values slightly smaller than K, there is always a period-adding scenario since for $H, T \approx K$ and $H < T$, we have $f'(T) = g'(T - H) \in (0, 1)$.

We now illustrate the above in two numerical bifurcation diagrams, namely for $H = 0.52 < H_{20} \approx 0.54$ and $H = 1.1 > H_{20}$. We begin with the case $H = 0.52 < H_{20}$ shown in Figure 9(A). For small, protective threshold values $T < H$, there is bistability between extinction and $x_+^* \approx 0.9$ (yellow background). At $T_1 = H$, a boundary-collision bifurcation occurs and replaces the LAS extinction equilibrium, to which initial conditions in $[m, M]$ converge, by an oscillatory attractor contained in I (green background). Hence, there are two regions of bistability for $T < T_2 = x_-^* \approx 0.57$. For $T \in (x_-^*, x_+^* + H)$, we observe that the equilibrium x_+^* is GAS. Finally, there are two period-adding BCBs at $T_3 = x_+^* + H \approx 1.43$ and $T_4 = K = 2$, the first one destabilizing the dynamics and the second one stabilizing the dynamics at the virgin stock level where harvesting no longer takes place.

Finally, let us consider the case $H = 1.1 > H_{20}$ in Figure 9(B). For small thresholds $T < H$, all ICs converge to the extinction equilibrium (grey background). For very protective thresholds $T > K$, harvesting is ceased and the virgin stock size K is GAS (light blue background). In between these two extremes (brown background), there are oscillatory population dynamics. More specifically, they emerge at $T = H$ in a boundary-collision bifurcation, which replaces extinction by complex dynamics. As T is increased, we observe a transition from apparently chaotic dynamics to a period-adding scenario. At $T = K$, the transition from oscillations to the GAS equilibrium K occurs in a period-adding BCB.

7. Average yield and harvest frequency. Here, we consider a more exploitation-oriented perspective by studying the average yield and harvest frequency as functions of the harvest control parameters. We first recall and extend some theoretical results before turning to numerical simulations.

A rigorous theoretical study of the MSY for the CC rule and the TCC rule, in the particular case of the Beverton–Holt model (2.2), can be found in [2]. Assuming that the management objective is the indefinite survival of the population, [2] concludes that, for the CC rule, the MSY is $H_{20} = f(\tilde{x}) - \tilde{x}$ and can be attained if and only if $x_0 \geq \tilde{x}$. However, if $x_0 < \tilde{x}$, then the optimal catch is $H_{\text{opt}} = f(x_0) - x_0 < H_{20}$. Recall that $\tilde{x}$ is the population size that sustains the MSY. That is, even for the optimal choice of the harvesting quota H, the MSY can be attained only for initial conditions exceeding the biomass level corresponding to MSY. For the TCC strategy with $T = f(\tilde{x})$, [2] shows that the MSY is equal to H_{20} and attainable for all ICs. In the following, as an expansion of the work in [2], we study the *average yield* $\overline{Y}$ and *harvest frequency* HF for the TCC rule applied to the Beverton–Holt model $f(x) = r\,x/(1+x)$, $r > 1$.

7.1. Analytical results. In some particular cases, it is possible to carry out an analytical study of both the average yield and the harvest frequency, e.g., when an equilibrium or a 2-cycle is an (essential) global attractor. First, assume that $T > K$ and $H < T$; then K is GAS. So for all ICs, after removing transients, we have $\overline{Y} = 0$ and $HF = 0$. That is, there is no harvesting in the long run. However, if $T \in [\tilde{x}, f(\tilde{x})]$ and $H = H_{20} < T$, then the equilibrium $\tilde{x}$ is an (essential) global attractor. In this case, for almost all ICs we have $\overline{Y} = H_{20}$ and $HF = 1$. That is, we can harvest at the MSY all the time.

Now we consider (H, T) values such that F has a 2-cycle which is an (essential) global attractor (see the region labeled with C in Figure 6(A)). The 2-cycle $\{x_1, x_2\}$ satisfies $f(x_1) < T < f(x_2)$, and thus $\overline{Y} = H/2$ and $HF = 1/2$. In this case, the average yield attains a local supremum at $H = H^* = (r-1)^2/(r+1)$ and $T = T^*$ $(g \circ f(T^* - H^*) = T^* - H^*)$. It is easy to prove that $H^* < H_{20} = (\sqrt{r} - 1)^2$, for all $r > 1$, which means that the MSY is not attainable. However, numerical simulations show that in spite of having harvest moratoria every other generation, the average yield can be close to H_{20} (see Figure 10(B)).

7.2. Numerical results. The presence of more complex dynamics or bistability makes it difficult to develop a rigorous analytical study of the average yield and harvest frequency. Thus, we study some numerical simulations for the population map $f(x) = 3x/(1+x)$, which help us to better understand the influence of T and H on $\overline{Y}$ and HF.

We begin by considering two different values of the threshold, namely $T = 0$ and $T = f(\tilde{x})$. For each of the fixed threshold values, we choose a random initial condition x_0 uniformly distributed in the interval $[0, \sup\{F(x) : x > 0\}] = [0, r - H] = [0, 3 - H]$. Then, we vary the fixed quota and for each value of H we run the system of equations (2.3)–(2.5) 650 times. After removing transients (600 iterations), we compute the average yield and harvest frequency for the last 50 iterations as follows:

$$\overline{Y} = \frac{1}{50} \sum_{n=601}^{650} Y_n, \quad HF = \frac{1}{50} \sum_{n=601}^{650} HF_n,$$

where, at generation $n \in \mathbb{N}$, $HF_n := 1$ if harvesting takes place and $HF_n := 0$ if there is no

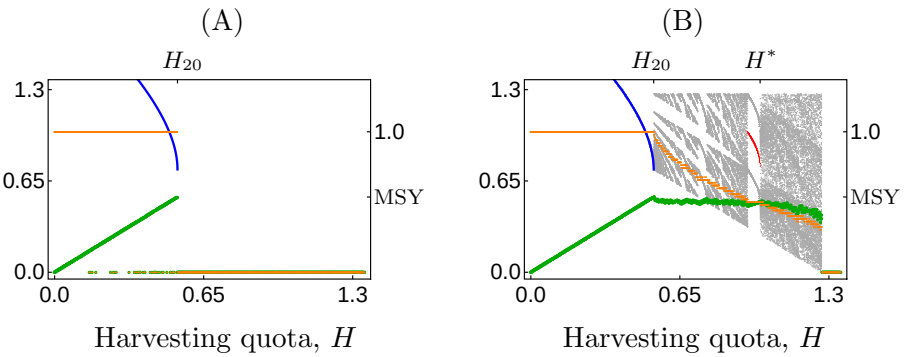

Figure 10. *Average yield (green lines) and harvest frequency (orange lines) for* (A) *the CC rule with* $T = 0$ *and* (B) *the TCC rule with* $T = f(\tilde{x})$*. The blue curve represents the LAS equilibrium* x_+^**. The red curve is the mean population size of the* 2*-cycle. The population bifurcation diagram is shown in grey. Simulations are for* (2.3)–(2.5) *with the Beverton–Holt map* $f(x) = 3x/(1+x)$*; see the main text for more details.*

harvesting.

First, the case $T = 0$ (CC rule) is presented in Figure 10(A). For quota values $H \leq H_{20}$, we observe bistability. If $x_0 < x_-^*$, the population perishes in a finite number of generations, so after removing transients we have $\overline{Y} = 0$ and $HF = 0$. If $x_0 > x_-^*$, the population converges to the LAS equilibrium x_+^*, so $\overline{Y} = H$ and $HF = 1$. When $H > H_{20}$, as 0 is GAS, after removing transients we have $\overline{Y} = 0$ and $HF = 0$. Therefore, Figure 10(A) illustrates that H_{20} is the MSY for the CC rule.

Second, the case $T = f(\tilde{x})$ is presented in Figure 10(B). We observe two main improvements in comparison with the CC rule. For $H \leq H_{20}$, the equilibrium x_+^* is a global attractor, so for all positive ICs, $\overline{Y} = H$ and $HF = 1$ (after removing transients). For $H \in (H_{20}, T)$, the population persists in an oscillatory manner and the average yield is smaller but quite close to MSY. Notice that for the CC rule it is quite risky to harvest at MSY, because $\overline{Y} = 0$ for all $H > H_{20}$. However, for $T = f(\tilde{x})$ and $H \in (H_{20}, H^*)$, $\overline{Y}$ remains very close to MSY and harvesting takes place at least every other generation as $HF \geq \frac{1}{2}$.

Now, we vary the threshold and fix the quota value $H = H_{20}$, which is the MSY for $T \in [0, f(\tilde{x})]$. In Figure 11, we show the average yield and harvest frequency as the threshold T increases, that is, as the harvesting strategy becomes more protective. If $T \in (0, \tilde{x})$, we observe bistability as for the CC rule, but the set of positive initial conditions for which $\overline{Y} = H_{20}$ and $HF = 1$ increases with increasing T (not explicitly illustrated in Figure 11). Moreover, for $T \in [H_{20}, \tilde{x})$, $\overline{Y} > 0$ for all positive ICs. The MSY is attainable for all positive ICs, if and only if $T \in [\tilde{x}, f(\tilde{x})]$, since $H_{20} < \tilde{x}$. For $T \in (f(\tilde{x}), K)$, the population persists in an oscillatory manner, and there are some generations of harvest moratoria and average yields smaller than H_{20}. When T is close to $K = 2$, the harvesting strategy is very conservative and the average yield is almost null.

8. Discussion and conclusions.

The TCC strategy combines CC harvesting with a threshold population size, below which harvesting is not allowed. We have shown in this paper that TCC is, not surprisingly, a protective strategy in the sense of promoting population persistence, where CC harvesting would lead to stock collapse. The CC strategy is risky, because

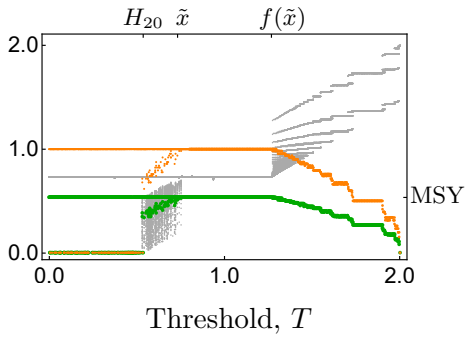

Figure 11. *Average yield (green lines) and harvest frequency (orange lines) for the TCC rule with a fixed quota $H = H_{20}$ and increasing harvesting thresholds. The population bifurcation diagram is shown in grey. Simulations are for (2.3)–(2.5) with the Beverton–Holt map $f(x) = 3x/(1 + x)$; see the main text for more details.*

the MSY quota is at a fold bifurcation point; increasing the quota slightly moves the fishery into the extinction regime. With TCC, the MSY is still obtained for the same quota value (as already shown in [2]), but for thresholds $T > H_{20}$ there is a "buffer" for harvest quotas $H \in (H_{20}, T)$ guaranteeing population persistence for all initial conditions even if the quota is beyond the MSY value that would lead to collapse under CC harvesting (see, e.g., Figures 7(A), 8, and 9). Remarkably, the average yield has been found to be almost as high as the MSY in this buffer range (see Figure 10(B)). Also, the harvest frequency remains close to 100% near the MSY value (see Figures 10(B) and 11). This observation coincides with a similar finding in a specific model of Baltic Sea cod [30]. TCC therefore seems viable for adaptive management, allowing quotas around and beyond the MSY, which typically comes with many problems for fisheries [39].

TCC also makes the fishery more resilient against perturbations of the population size, because it guarantees deterministic persistence for all initial conditions or diminishes the set of initial conditions converging to the extinction state. Taken together with the buffer zone for enhanced quota levels, TCC is remarkably protective to the stock while providing high yields with almost no fishing moratoria. TCC thus remedies many of the well-known and notorious problems of the CC strategy (high extinction risk) and pure threshold harvesting (high yield variability and fishery closures).

In TCC, it is possible that the population size after harvesting falls below the threshold. This could seem strange if the threshold is viewed as a minimum below which the population size should not fall. However, our results show that despite this possibility TCC is still beneficial for both population conservation and sustained yield. Only when the harvesting quota is so high that it exceeds the threshold ($H > T$) is population extinction possible. To avoid population sizes falling below the threshold, one could devise alternative strategies with multiple thresholds. An example is the PTCC rule, where the escapement is at least as large as the threshold [40].

For certain control parameter values, TCC can induce oscillations in population size. In the absence of harvesting, we assume in this paper undercompensatory population growth like in the Beverton–Holt map, which always yields stable dynamics and not even damped

oscillations. We are not aware of many simple control rules like TCC that can destabilize Beverton–Holt dynamics. The oscillations could be formed by alternating phases of population size decay (overharvesting above threshold) and recovery (population growth below threshold). Hence, TCC induces an effect similar to overcompensation, i.e., reduced population growth at large population sizes, which is well known to induce oscillations.

The model in this paper can exhibit rich and complex dynamics. In some dynamical regimes, we know for sure that oscillations exist (see Figure 5(A)), while in other cases there may be long transients (see Figure 7(A)). If the long transients are actually oscillatory attractors, there is tristability. In practice, it might not matter whether the oscillations are transient when they are on a long time scale [24]. In parameter regions with an attracting 2-cycle (see Figure 7(B)), we find a hydra effect. This effect cannot occur in nonoscillatory mode (for $T < K$) since the attracting fixed points decrease as harvesting parameters increase.

Probably the most notorious feature of the TCC rule from a dynamical systems point of view is the discontinuity at the harvesting threshold. This makes the TCC rule a discontinuous piecewise-smooth map. We observe a wide range of dynamic phenomena ranging from boundary-collision bifurcations and basin boundary metamorphoses over multistability and homoclinic orbits to BCBs. The latter come in the form of existence and period-adding BCBs. The boundary-collision bifurcations come in the form of both boundary crises (Figures 7(A)–(B), 8(A), and 9(A)–(B)) and interior crises (Figure 8(C)). The nonsmooth bifurcations are related to invariant sets colliding with the break point, which is given by the harvesting threshold. Reference [5] also studied a discontinuous one-dimensional map with no harvesting below a threshold but with proportional (rather than CC) harvesting above the threshold. Reference [5] found BCBs as well. Note that related control rules like pure threshold harvesting, CC, proportional harvesting, or PTCC are continuous, so their dynamical behavior (see, e.g., [2, 40, 29]) is less rich.

Regarding nonsmooth bifurcations in discontinuous piecewise-smooth one-dimensional dynamical systems, we also find some interesting features. First, it is mentioned in [3] that although we usually study bifurcations of attractors, bifurcations of other invariant sets can also essentially influence the dynamics and are worth being investigated. This is the case for the existence BCB of the unstable 2-cycle in Figure 8(C). However, we observe in Figure 7(A) that for smaller values of the threshold T, the same type of bifurcation does not have a significant influence on the dynamics. Second, there are nonsmooth bifurcations for the TCC map which appear in a manner different from the one described in [3]. For instance, basin boundary metamorphoses and boundary-collision bifurcations occur without the existence of a homoclinic orbit (we find homoclinic orbits at period-adding BCBs; see Figures 3 and 4). Basin boundary metamorphoses are simple; that is, they do not involve fractal basins of attraction as in [23]. Boundary-collision bifurcations are due to the nonsmoothness of the TCC map, which is not the case for PTCC (see section IV in [40]). There are also some BCBs different from those described in [3], for instance the existence BCB. Third, we observe typical sequences of bifurcations in one-parameter bifurcation diagrams, the period-adding scenario (see Figures 7 to 9), and an apparently truncated skew tent map scenario (see Figure 8). The last scenario does not exactly follow the structure defined in section 3.2 of [3], because it is not possible to have a degenerated flip bifurcation since $(F^{2k})'(x) > 0$ for all $x > 0$.

This paper highlights the protective function of thresholds and the complex dynamics

that are possible due to a threshold-induced discontinuity. TCC is a very simple harvesting strategy, but it could provide insights for more complicated control rules. Thresholds form an important part of current harvest control rules [12, 50, 18]. While many of them are designed to be a continuous function, in practice there could be a discontinuous jump in the harvesting escapement around the threshold level for a number of reasons. On the one hand, one should have in mind that population size estimates are uncertain and often delayed. On the other hand, thresholds could prompt certain behaviors of fishermen or certain responses of institutions. It will be interesting to account for such aspects as well as further model variants such as overcompensatory population dynamics, depensation, ecosystem effects, and age or spatial structure.

Appendix A.

A.1. Proofs of Propositions 4.1 and 4.2. We begin providing the following result on the existence of positive fixed points of the map F defined in (2.4). Throughout this subsection, let $x_T > 0$ be the unique solution of $f(x) = T$.

Proposition A.1. *Assume that f satisfies* **(A)**. *Denote by $\tilde{x}$ the unique solution of $f'(x) = 1$. Then the following hold:*

(i) *If $T > K$, then K is the unique positive equilibrium of F for all $H > 0$.*
(ii) *If $f(\tilde{x}) \le T < K$, then $x_+^* \in [\tilde{x}, K)$ is the unique positive fixed point of F if and only if $H \le H_{10} = T - \widetilde{x_+^*}$, where $f(\widetilde{x_+^*}) = T$.*
(iii) *If $0 < T < f(\tilde{x})$, then the following hold:*
  (a) *If $H < H_{12} = T - \widetilde{x_-^*}$, where $f(\widetilde{x_-^*}) = T$, then $x_+^* \in [\tilde{x}, K)$ is the unique positive fixed point of F.*
  (b) *If $H_{12} \le H < H_{20} = f(\tilde{x}) - \tilde{x}$, then F has two positive fixed points $x_-^* < \tilde{x} < x_+^*$.*
  (c) *If $H = H_{20}$, then $\tilde{x}$ is the unique positive equilibrium of F.*

In the rest of the cases, 0 is the unique fixed point of F.

Proof of Proposition A.1. From the definition of the map F in (2.4), we have the following:

If $T > K = f(K)$ (as f is an increasing function, $x_T > K$), then $F(x) = f(x)$ for all $x \in (0, x_T)$, and $F(x) = g(x) = f(x) - H < x - H < x$ for all $x > x_T$.

If $T < K = f(K)$ (as f is a strictly increasing function, $x_T < K$), then $F(x) = f(x) > x$ for all $x \in (0, x_T)$, and $F(x) = 0$ or $F(x) = g(x) = f(x) - H$ for all $x > x_T$.

Thus, we can conclude that K is a fixed point of F if and only if $T > K$, and for $T < K$ the positive fixed points of F are the ones of g.

Since $g'(x) = f'(x) > 0$ and $g''(x) = f''(x) < 0$, by the mean value theorem, g can have at most two positive fixed points $x_-^* \le \tilde{x} \le x_+^*$. Now, the proofs of (ii) and (iii) follow easily. ∎

The proof of Proposition 4.1 follows from Proposition A.1 and the following technical result, which is a simple generalization of Lemma 1 in [6]. Note that this result was established in [40], in order to prove stability of fixed points for the PTCC harvesting strategy.

Lemma A.2. *Let $h : (a, b) \longrightarrow (a, b)$ be a continuous function defined on a real interval (a, b) $(-\infty \le a < b \le \infty)$, such that h has a unique fixed point x^* with $x < h(x) < x^*$ for all $x \in (a, x^*)$, and $a < h(x) < x$ for all $x \in (x^*, b)$. Then, x^* is a global attractor of h.*

Proof of Proposition 4.1. The existence of the different fixed points of F is given in Proposition A.1.

To prove (i), we apply Lemma A.2 to the map $F_{|(0,x_T)} = f_{|(0,x_T)}$; then K is a global attractor in $(0, x_T)$. If $H < T$, then $0 < g(x_T) < F(x) = f(x) - H < x - H < x$ for all $x > x_T > K$ and $g(x_T) = f(x_T) - H = T - H < T$. Thus, all initial conditions $x_0 > x_T$ enter in $(0, x_T)$ in finite time and converge to K. If $H \geq T$, then $g(x) = 0$ for all $x \in [x_T, M] = [m, M]$. Moreover, for all $x > M > x_T$, the proof follows as in the case $H < T$.

Now, we consider the cases (ii) and (iii)(a); from Proposition A.1 we know that x_+^* is the unique positive fixed point of F. Moreover, $x_+^* = x_T$ if $H = H_{10}$ since $F(x_T) = g(x_T) = f(x_T) - H_{10} = T - (T - x_T) = x_T$, and $x_+^* \in (x_T, K)$ otherwise. The proof of case (ii) with $H = H_{10}$ is a direct consequence of the following conditions fulfilled by f and g: $F(x) = f(x) > x$ for all $0 < x < x_T < K$; $F(x) = g(x) < x$ for all $x > x_T$; and $T = f(x_T) > F(x_T) = g(x_T)$. In the remainder cases, we apply Lemma A.2 to the map $F_{|(x_T,\infty)} = g_{|(x_T,\infty)}$, and we have that x_+^* is GAS in (x_T, ∞). For all $x \in (0, x_T)$, $F(x) = f(x) > x$; and since $f(x_T) > g(x_T)$, we can conclude that all initial conditions in $(0, x_T)$ enter in (x_T, ∞) in finite time and thus converge to x_+^*.

The proofs of cases (iii)(b) and (iii)(c) are easier, so we leave it to the reader. ∎

Finally, we provide the proof of Proposition 4.2, which is straightforward.

Proof of Proposition 4.2. In all cases, since $T \leq K = f(K)$, we have $F(x) = f(x) > x$ for all $x \in (0, x_T)$. In addition, $F(x) = \max\{0, g(x)\}$ for all $x \geq x_T$. In cases (a), (b), and (c), for all $x \geq x_T$, $g(x) = f(x) - H < x$. While in case (d), $g(x) < x$ if and only if $x \in [x_T, x_-^*) \cup (x_+^*, \infty)$.

Consequently, it is clear that there exists an invariant or strictly mapped into itself interval $I = [\max\{0, g(x_T)\}, f(x_T)] = [\max\{0, f(x_T) - H\}, T] = [\max\{0, T - H\}, T]$. It also follows that all initial conditions enter in I in finite time in cases (a), (b), and (c). However, in case (d), we can assert that just the ICs in $(0, x_-^*)$ enter in I in finite time since from Proposition 4.1 we have that (x_-^*, ∞) is the basin of attraction of x_+^*.

Finally, it remains to prove that I does not contain any positive fixed point. The cases (a), (b), and (c) are trivial since under the corresponding conditions the map F has no positive fixed points. In case (d), the positive fixed points of F are $x_-^* < x_+^*$, and the statement follows since $H > H_{\text{oscill}}$ implies that $T < x_-^*$. ∎

REFERENCES

[1] P. A. Abrams, *When does greater mortality increase population size? The long history and diverse mechanisms underlying the hydra effect*, Ecol. Lett., 12 (2009), pp. 462–474.

[2] Z. AlSharawi and M. B. H. Rhouma, *The Beverton–Holt model with periodic and conditional harvesting*, J. Biol. Dyn., 3 (2009), pp. 463–478.

[3] V. Avrutin, L. Gardini, I. Sushko, and F. Tramontana, *Continuous and Discontinuous Piecewise-Smooth One-Dimensional Maps*, World Scientific, Singapore, 2019.

[4] V. Avrutin and I. Sushko, *A gallery of bifurcation scenarios in piecewise smooth* 1*D maps*, in Global Analysis of Dynamic Models in Economics and Finance, G. I. Bischi, C. Chiarella, and I. Sushko, eds., Springer, Berlin, 2013, pp. 369–395.

[5] G. I. Bischi, F. Lamantia, and F. Tramontana, *Sliding and oscillations in fisheries with on–off harvesting and different switching times*, Commun. Nonlinear Sci. Numer. Simul., 19 (2014), pp. 216–229.
[6] E. Braverman and E. Liz, *Global stabilization of periodic orbits using a proportional feedback control with pulses*, Nonlinear Dynam., 67 (2012), pp. 2467–2475.
[7] D. S. Butterworth, *A suggested amendment to the harvesting strategy used at ICSEAF to specify hake TAC levels*, Coll. Scient. Pap. Int. Commn S.E. Atl. Fish., 14 (1997), pp. 101–108.
[8] C. W. Clark, *Mathematical Bioeconomics. The Optimal Management of Renewable Resources*, Wiley, New York, 1976.
[9] C. W. Clark, *Bioeconomics*, in Theoretical Ecology: Principles and Applications, R. M. May, ed., Blackwell, Oxford, UK, 1981, pp. 387–418.
[10] W. G. Clark and S. R. Hare, *A conditional constant catch policy for managing the Pacific halibut fishery*, N. Am. J. Fish. Manag., 24 (2004), pp. 106–113.
[11] R. Deriso, *Risk averse harvesting strategies*, in Resource Management, M. Mangel, ed., Springer, Berlin, 1985, pp. 65–73.
[12] J. J. Deroba and J. R. Bence, *A review of harvest policies: Understanding relative performance of control rules*, Fish. Res., 94 (2008), pp. 201–233.
[13] M. di Bernardo, C. J. Budd, A. R. Champneys, and P. Kowalczyk, *Piecewise-Smooth Dynamical Systems*, Springer, London, 2008.
[14] M. di Bernardo, C. J. Budd, A. R. Champneys, P. Kowalczyk, A. B. Nordmark, G. O. Tost, and P. T. Piiroinen, *Bifurcations in nonsmooth dynamical systems*, SIAM Rev., 50 (2008), pp. 629–701.
[15] S. Engen, R. Lande, and B.-E. Sæther, *Harvesting strategies for fluctuating populations based upon uncertain population estimates*, J. Theoret. Biol., 186 (1997), pp. 201–212.
[16] D. Franco and F. M. Hilker, *Adaptive limiter control of unimodal population maps*, J. Theoret. Biol., 337 (2013), pp. 161–173.
[17] D. Franco and F. M. Hilker, *Stabilizing populations with adaptive limiters: Prospects and fallacies*, SIAM J. Appl. Dyn. Syst., 13 (2014), pp. 447–465.
[18] R. Froese, T. A. Branch, A. Proelss, M. Quaas, K. Sainsbury, and C. Zimmermann, *Generic harvest control rules for European fisheries*, Fish Fish. (Oxf), 12 (2011), pp. 340–351.
[19] J. M. Fryxell, A. R. E. Sinclair, and G. Caughley, *Wildlife Ecology, Conservation, and Management*, 3rd ed., Wiley Blackwell, Chichester, UK, 2014.
[20] J. M. Fryxell, I. M. Smith, and D. H. Lynn, *Evaluation of alternate harvesting strategies using experimental microcosms*, OIKOS, 111 (2005), pp. 143–149.
[21] L. Gardini, V. Avrutin, and I. Sushko, *Codimension-2 border collision bifurcations in one-dimensional discontinuous piecewise smooth maps*, Internat. J. Bifur. Chaos Appl. Sci. Engrg., 24 (2014), 1450024.
[22] C. Grebogi, E. Ott, and J. A. Yorke, *Chaotic attractors in crisis*, Phys. Rev. Lett., 48 (1982), pp. 1507–1510.
[23] C. Grebogi, E. Ott, and J. A. Yorke, *Metamorphoses of basin boundaries in nonlinear dynamical systems*, Phys. Rev. Lett., 56 (1986), pp. 1011–1014.
[24] A. Hastings, *Timescales and the management of ecological systems*, Proc. Natl. Acad. Sci. USA, 113 (2016), pp. 14568–14573.
[25] R. Hilborn, *The evolution of quantitative marine fisheries management* 1985–2010, Nat. Resour. Model., 25 (2012), pp. 122–144.
[26] R. Hilborn and C. J. Walters, *Quantitative Fisheries Stock Assessment: Choice, Dynamics and Uncertainty*, Chapman & Hall, London, 1992.
[27] F. M. Hilker and E. Liz, *Harvesting, census timing and "hidden" hydra effects*, Ecol. Complex., 14 (2013), pp. 95–107.
[28] F. M. Hilker and E. Liz, *Proportional threshold harvesting in discrete-time population models*, J. Math. Biol., 79 (2019), pp. 1927–1951.
[29] F. M. Hilker and E. Liz, *Threshold harvesting as a conservation or exploitation strategy in population management*, Theor. Ecol., 13 (2020), pp. 519–536.
[30] O. Hjerne and S. Hansson, *Constant catch or constant harvest rate?: The Baltic Sea cod (*Gadus morhua *L.) fishery as a modelling example*, Fish. Res., 53 (2001), pp. 57–70.

[31] ICES, *Report of the ICES Advisory Committee on Fishery Management, Part* 1, vol. 255 of ICES Cooperative Research Report, 2002.
[32] ICES, *Report of the Study Group on Management Strategies (SGMAS),* 23–27 *January* 2006*, ICES Headquarters*, vol. ICES CM 2006/ACFM:15, 2006.
[33] ICES, *Report of the Arctic Fisheries Working Group (AFWG)*, vol. ICES CM 2018/ACOM:06. Ispra: ICES, 2018.
[34] N. Jonzén and P. Lundberg, *Temporally structured density dependence and population management*, Ann. Zool. Fenn., 36 (1999), pp. 39–44.
[35] V. Kaitala, N. Jonzén, and K. Enberg, *Harvesting strategies in a fish stock dominated by low-frequency variability: The Norwegian spring-spawning herring (*Clupea harengus*)*, Mar. Resour. Econ., 18 (2003), pp. 263–274.
[36] C. J. Kelly and E. A. Codling, *"Cheap and dirty" fisheries science and management in the North Atlantic*, Fish. Res., 79 (2006), pp. 233–238.
[37] D. A. Kroodsma, J. Mayorga, T. Hochberg, N. A. Miller, K. Boerder, F. Ferretti, A. Wilson, B. Bergman, T. D. White, B. A. Block, P. Woods, B. Sullivan, C. Costello, and B. Worm, *Tracking the global footprint of fisheries*, Science, 359 (2018), pp. 904–908.
[38] R. Lande, B.-E. Sæther, and S. Engen, *Threshold harvesting for sustainability of fluctuating resources*, Ecology, 78 (1997), pp. 1341–1350.
[39] P. A. Larkin, *An epitaph for the concept of maximum sustained yield*, Trans. Am. Fish. Soc., 106 (1977), pp. 1–11.
[40] E. Liz and C. Lois-Prados, *Dynamics and bifurcations of a family of piecewise smooth maps arising in population models with threshold harvesting*, Chaos, 30 (2020), pp. 1–16.
[41] D. Ludwig, *Management of stocks that may collapse*, OIKOS, 83 (1998), pp. 397–402.
[42] P. M. Mace, *Relationships between common biological reference points used as thresholds and targets of fisheries management strategies*, Can. J. Fish. Aquat. Sci., 51 (1994), pp. 110–122.
[43] S. L. Maxwell, R. A. Fuller, T. M. Brooks, and J. E. M. Watson, *The ravages of guns, nets and bulldozers*, Nature, 536 (2016), pp. 143–145.
[44] S. A. Murawski and J. S. Idoine, *Yield sustainability under constant-catch policy and stochastic recruitment*, Trans. Am. Fish. Soc., 118 (1989), pp. 349–367.
[45] S. A. Murawski and F. M. Serchuk, *Mechanized shellfish harvesting and its management: The offshore clam fishery of the eastern United States*, in Marine Invertebrate Fisheries: Their Assessment and Management, J. F. Caddy, ed., Wiley, New York, 1989, pp. 479–506.
[46] H. E. Nusse and J. A. Yorke, *Border-collision bifurcations including "period two to period three" for piecewise smooth systems*, Phys. D, 57 (1992), pp. 39–57.
[47] Pacific Fishery Management Council, *Pacific Coast Groundfish Fishery Management Plan for the California, Oregon and Washington Groundfish Fishery*, Pacific Fishery Management Council, Portland, OR, 2016.
[48] A. Panchuk, I. Sushko, and F. Westerhoff, *A financial market model with two discontinuities: Bifurcation structures in the chaotic domain*, Chaos, 28 (2018), 055908.
[49] D. G. Pazhayamadom, C. J. Kelly, E. Rogan, and E. A. Codling, *Decision interval cumulative sum harvest control rules (DI-CUSUM-HCR) for managing fisheries with limited historical information*, Fish. Res., 171 (2015), pp. 154–169.
[50] A. E. Punt, *Harvest control rules and fisheries management*, in Handbook of Marine Fisheries Conservation and Management, R. Q. Grafton, R. Hilborn, D. Squires, M. Tait, and M. J. Williams, eds., Oxford University Press, Oxford, UK, 2010, pp. 582–594.
[51] T. J. Quinn, R. Fagen, and J. Zheng, *Threshold management policies for exploited populations*, Can. J. Fish. Aquat. Sci., 47 (1990), pp. 2016–2029.
[52] J. Segura, F. M. Hilker, and D. Franco, *Adaptive threshold harvesting and the suppression of transients*, J. Theoret. Biol., 395 (2016), pp. 103–114.
[53] J. Segura, F. M. Hilker, and D. Franco, *Degenerate period adding bifurcation structure of one-dimensional bimodal piecewise linear maps*, SIAM J. Appl. Math., 80 (2020), pp. 1356–1376.
[54] A. R. E. Sinclair, J. M. Fryxell, and G. Caughley, *Wildlife Ecology, Conservation, and Management*, 2nd ed., Wiley Blackwell, Oxford, UK, 2006.

[55] D. W. Skagen, *Management strategies for reducing variation in annual yield: When can they work?*, ICES J. Mar. Sci., 64 (2007), pp. 698–701.
[56] E. M. Steiner, K. R. Criddle, and M. D. Adkinson, *Balancing biological sustainability with the economic needs of Alaska's sockeye salmon fisheries*, N. Am. J. Fish. Manag., 31 (2011), pp. 431–444.
[57] I. Sushko, L. Gardini, and V. Avrutin, *Nonsmooth one-dimensional maps: Some basic concepts and definitions*, J. Difference Equ. Appl., 22 (2016), pp. 1816–1870.